

Chapter 9

Evidence for Late Devonian (Kellwasser) anoxic events in the Great Basin, western United States

David Bond* and Paul B. Wignall

School of Earth Sciences, University of Leeds, Leeds LS2 9JT, UK

Abstract

The Frasnian-Famennian (Late Devonian) mass extinction has often been related to the development of the Kellwasser anoxic events in Europe and North Africa but the synchronous development of the anoxia has not been reported from the Great Basin of the western United States. An integrated sedimentological, palaeoecological, and pyrite petrographic study has been undertaken on a range of F-F boundary sections from Nevada and Utah spanning a spectrum of carbonate and clastic depositional environments from distal basin, base-of-slope, mid-slope, and intra-shelf basin settings. These reveal a range of facies from oxic strata, fully bioturbated and lacking any pyrite, to euxinic strata characterised by fine lamination and pyrite framboid populations of small size and narrow size range. Oxygen-restricted deposition is seen in all sections at various times, but the only interval characterised by basin-wide euxinic conditions occurs at the end of the Frasnian Stage late in the *linguiformis* Zone. This is the peak of the F-F mass extinction and it is also contemporaneous with the Upper Kellwasser Horizon of Europe. The study therefore reinforces the claim that the mass extinction coincides with the global development of marine anoxia. Shallow-water sections were not studied but slope and base-of-slope sections record many sediment-gravity flows that transported an allochthonous fauna into deeper-water settings. This shallow-water fauna temporarily disappears late in the *linguiformis* Zone perhaps indicating the development of oxygen-restriction in shallow-water settings. Intriguingly the condensed, deepest water sections from the Woodruff basin record somewhat higher oxygenation levels than the contemporaneous slope sections. The most oxygen-restricted conditions may therefore have occurred in a mid-water oxygen-minimum zone that expanded its vertical range both upwards and downwards and became sulphidic late in the *linguiformis* Zone.

1. Introduction

The extinction losses near the Frasnian-Famennian (F-F, Late Devonian) boundary constitute one of the “big 5” crises of the fossil record (e.g. Raup and Sepkoski, 1982; Sepkoski, 1996). Several causal mechanisms have been proposed, and marine anoxia is widely regarded to have played a role in many of them. The extinctions are associated with two discrete anoxic events (House, 1985; Casier, 1987; Walliser et al., 1989; Goodfellow et al., 1989; Buggisch, 1991; Becker, 1993). These events are manifest in Germany as bituminous limestones known as the Lower and Upper Kellwasser horizons that developed in the Late *rhenana* and late in the *linguiformis* conodont zones, respectively (Buggisch, 1972; Schindler, 1990; Walliser, 1996). Elsewhere in Europe, the intensity and duration of anoxic

*Corresponding author. Fax: +44-113-343-5259. *E-mail address*: d.bond@earth.leeds.ac.uk (D. Bond).

facies varies according to water depth. For instance in Poland and France, anoxia is postulated to have developed during the Frasnian on basin slopes, before developing in shelf and shallow-water environments in the latest *linguiformis* Zone (Bond et al., 2004). Implicit in the anoxia kill hypothesis is the need for globally synchronous and widespread anoxia (e.g. House, 1985). Crucially therefore, the fact that the latest Frasnian event (corresponding to the Upper Kellwasser Horizon of Germany) was widespread and simultaneous in its development, increases the likelihood that it was a direct cause of the marine mass extinction. Age-equivalent anoxic facies are also known over a wide area from Morocco to the subpolar Urals (Wendt and Belka, 1991; Racki et al., 2002; Yudina et al., 2002).

Although the Kellwasser facies in Europe present clear evidence for widespread anoxia, previous work in the Great Basin of the western United States has suggested that the anoxic interval significantly pre-dated the F-F boundary. Furthermore, the F-F boundary interval may in fact record oxic deposition, perhaps as a result of relative sea-level fall (Bratton et al., 1999). Thus, the latest Frasnian anoxic event may have been of regional (i.e. European and North Africa) rather than global extent. This seriously undermines the role of anoxia in the mass extinction.

The oxygenation history proposed by Bratton et al. (1999) was based on a range of geochemical redox indicators, principally trace metal indices, from outcrop sections in the deserts of Nevada and Utah. A new approach for analysing palaeo-oxygenation levels has been applied to the sections originally used in the Bratton et al. (1999) study (Coyote Knolls and Whiterock Canyon), and additional sections (Devils Gate, Northern Antelope Range, Tempiute Mountain, and Warm Springs). In this study, we document the late Frasnian–early Famennian oxygenation history of the Great Basin, using integrated techniques of pyrite framboid and sedimentary fabric analysis. Unlike many geochemical indices, both these rock attributes are preserved even in heavily-weathered strata (e.g. Lüning et al., 2003). It is hoped to clarify the F-F redox record of the United States, and thus to determine how widespread the anoxic facies were. Comparisons with the timing of anoxia in Europe are made, in order to address the question of whether anoxia was implicated in the Late Devonian mass extinction.

2. Regional geology of the Great Basin

The Great Basin Devonian outcrops of Nevada and Utah record deposition adjacent to a foreland basin (Fig. 1). This formed the central part of a large continental carbonate shelf extending northwards from Mexico to western Canada, along the western edge of Laurasia (Sandberg and Poole, 1977; Sandberg et al., 1989; Morrow, 2000), located at 5–10° N (Scotese and McKerrow, 1990). The sections record deposition in two basins, the Pilot and the Woodruff basins, separated by the proto-Antler forebulge (Sandberg et al., 2003) (Fig. 2). To the east of the forebulge, the Pilot Basin was a rapidly subsiding, deep-water intra-shelf Basin with an infill dominated by siltstones, thin micrites, and sandy turbidites (Sandberg et al., 1989). To the west of the forebulge was a slope, and the deep Woodruff Basin in which debris-flow carbonates, turbidites, siltstones, mudstones, and cherts accumulated (Sandberg et al., 2003). During the Famennian and Early Carboniferous, the Antler Orogeny caused basinal sediments to be thrust eastwards onto the slope and outer shelf, resulting in tectonic interfingering of shallow and deep-water deposits along the Roberts

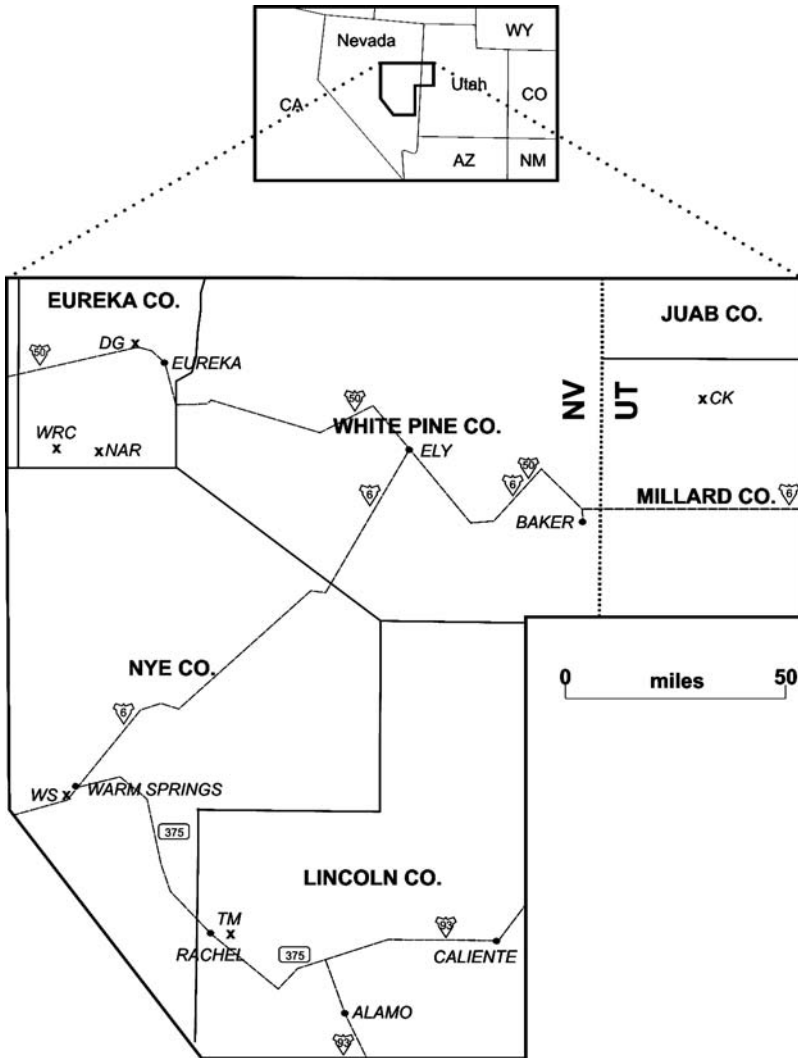


Figure 1. Locality map of study sections in the western United States, showing principal towns and highways. CK = Coyote Knolls; DG = Devils Gate; NAR = Northern Antelope Range; TM = Tempiute Mountain; WRC = Whiterock Canyon; WS = Warm Springs.

Mountains Thrust, which runs along the western edge of the Pilot Basin (Sandberg and Poole, 1977; Sandberg et al., 1989). The studied sections are representative of a variety of depositional settings, and are presented from east to west, from the intra-shelf Pilot Basin, across the proto-Antler forebulge, to the slope and basinal sites of the Woodruff Basin (Fig. 2; Appendix A). Slope deposits are well exposed in the well-known Devils Gate section while further west the Northern Antelope Range and Tempiute Mountain sections expose middle to basal slope/Basin floor deposits. Warm Springs and Whiterock Canyon expose the deepest water sections of this study, from the Basin floor of the Woodruff Basin

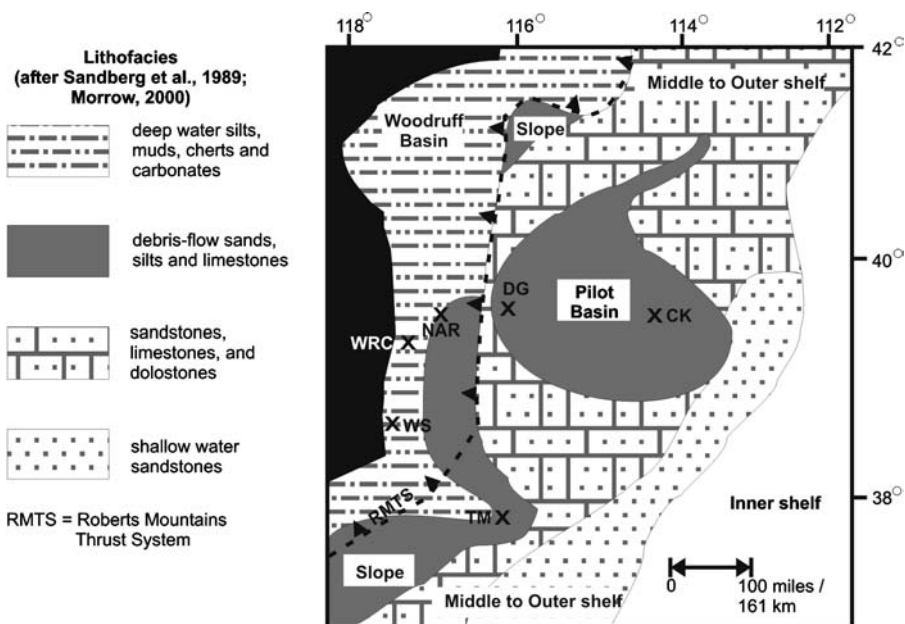


Figure 2. Lithofacies and palaeogeography of the Great Basin during the Frasnian-Famennian interval showing location of sections studied in this chapter. Modified from Sandberg et al. (1989) and Morrow (2000). Note movement on the Roberts Mountains thrust (hachured) has not been fully restored, thus foreshortening the shelf-basin transition in some areas (section abbreviations as in Fig. 1).

(Sandberg et al., 1997, 2002, 2003; Morrow, 2000; see Fig. 2). The sections vary considerably in thickness, depending on their depositional environment: basinal sections of the Woodruff Basin being thinner than both the slope sections and the expanded Pilot Basin section of Coyote Knolls (Fig. 3).

3. Analytical procedure and rationale

Oxygenation levels recorded in the F-F boundary sections were assessed using two independent criteria: sediment fabric (i.e. presence of lamination and/or degree of bioturbation) and pyrite framboid size populations. Boundary sections were logged in detail with care taken to identify the presence (or absence) of fine lamination/bioturbation features. Field determinations were supplemented by petrographic analysis of thin sections and examination of polished blocks. Burrow size is known to decrease along a transition from oxic to dysoxic conditions, and burrows disappear completely in anoxic conditions (Savrda and Bottjer, 1986). Euxinic conditions (defined by the presence of a sulphidic lower water column) are also associated with laminated sediment, but it is not possible to distinguish anoxic conditions, where anoxia is only developed at the seabed, from euxinic conditions using sediment fabric alone. This is better achieved from analysis of pyrite framboid populations.

Polished blocks were examined under backscatter SEM at a magnification of $\times 2670$, to determine the pyrite content and, where present, the size distribution of pyrite framboid

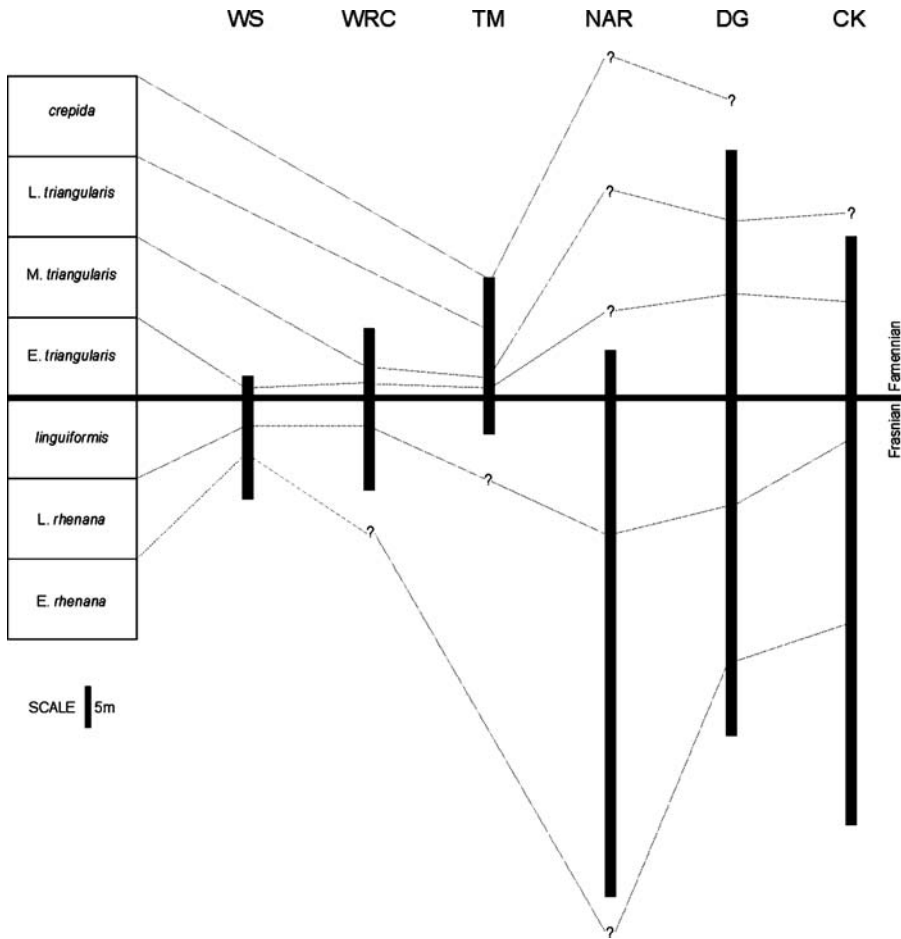


Figure 3. Correlation of study sections (abbreviations as in Fig. 1), showing the development of thinner, basal sections in the western outcrops, and thicker, slope sections to the east.

populations (Fig. 4). Where possible, at least 100 framboids were measured per sample although in some of the more carbonate-rich lithologies the pyrite content is low and the density of framboids consequently too low to achieve the desired 100 framboid sample size (see Appendix B).

Framboids form as an aggregate of iron monosulphide microcrystals, and Wilkin and Barnes (1996, 1997) proposed a four-stage model for their formation. Firstly, iron monosulphide microcrystals nucleate. These then react to form greigite (Fe_3S_4), followed by aggregation of greigite microcrystals (due to magnetic attraction) to form spherical framboids. Finally, greigite is replaced by pyrite to form pyrite framboids. The reaction of iron monosulphide to form greigite requires weakly oxidising conditions, in order to supply elemental sulphur, whereas the first and fourth stages both require reducing conditions (Raiswell, 1982; Canfield and Thamdrup, 1994). Thus, the environment where pyrite framboids can form is tightly constrained to the close proximity of the redox boundary.

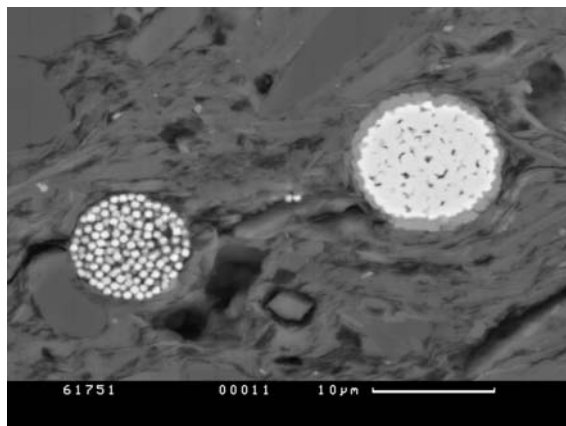


Figure 4. SEM photograph of pyrite framboids from the Devils Gate section (bed 4). Note that the framboid on the right of the picture exhibits an oxidised rim but still retains the framboid morphology.

Framboids cease to grow in the more intensely anoxic conditions of the underlying sulphate-reduction zone, where more slowly growing crystalline pyrite forms (Wilkin and Barnes, 1997). If bottom waters become anoxic (i.e. euxinic conditions develop), then framboids develop in the water column but are unable to achieve diameters much larger than 5 μm before they sink below the Fe-reduction zone and cease to grow (Wilkin et al., 1996). For example, in modern Black Sea sediments, deposited in the type example of a euxinic basin, framboids rarely exceed 6 μm in diameter (Muramoto et al., 1991). Thus, euxinic conditions produce populations of tiny framboids with a narrow size range. In contrast, in dysoxic environments, where framboids form in surficial sediments, size is largely governed by the local availability of reactants and the framboids are larger and more variable in size (Wilkin et al., 1996).

In a detailed study of a range of modern depositional environments, Wilkin et al. (1996) found that framboids formed in a euxinic water column (such as the Black Sea) have a mean diameter, standard deviation, and maximum framboid diameter that are smaller than those framboids formed under oxygenated or dysoxic water columns. Wilkin et al. (1996) suggested that, because framboid size is preserved throughout diagenesis and lithification, the technique could also be applied to ancient sediments. Subsequently, Wignall and Newton (1998) found a close correspondence between the framboid size parameters noted above and water column oxygenation levels determined using palaeoecological criteria. They confirmed that pyrite framboid analyses can additionally provide a subtle indicator of environmental stability (Wignall and Newton, 1998).

Many lower dysaerobic biofacies record variable oxygenation regimes in which long-term euxinic conditions are punctuated by brief seafloor oxygenation events that allowed colonisation by a benthic pioneer fauna (Hallam, 1980; Wignall and Myers, 1988). Thus, there is often a dichotomy between geochemical evidence from lower dysaerobic facies which records long-term (average) depositional conditions and palaeoecological evidence which can record shorter-term (atypical) events (Raiswell et al., 2001). Such facies have a distinctive pyrite framboid size signature dominated by small, syngenetic populations formed

in euxinic conditions but with the addition of rare, larger (>5 μm diameter) framboids formed within the sediment during brief intervals of seafloor oxygenation (Wignall and Newton, 1998; Table 1). It is therefore useful to measure maximum framboid diameter (MFD), provided a sufficiently large sample size is obtained, as this can provide a further subtle indicator of transient oxygenation events.

A great advantage of pyrite framboid analysis over other geochemical proxies for ancient redox levels is the ability of framboids to withstand both diagenetic alteration and weathering. Once formed, framboids are not observed to grow or accrete in modern environments, and anoxic conditions are generally characterised by the growth of crystalline or amorphous forms of pyrite. On exposure, framboids and other sedimentary pyrite are weathered to iron oxy-hydroxides, but this only involves the pseudomorphing of the framboids; it is still possible to measure framboid size even in intensely weathered samples (Fig. 4).

4. Great Basin sections

4.1. Coyote Knolls

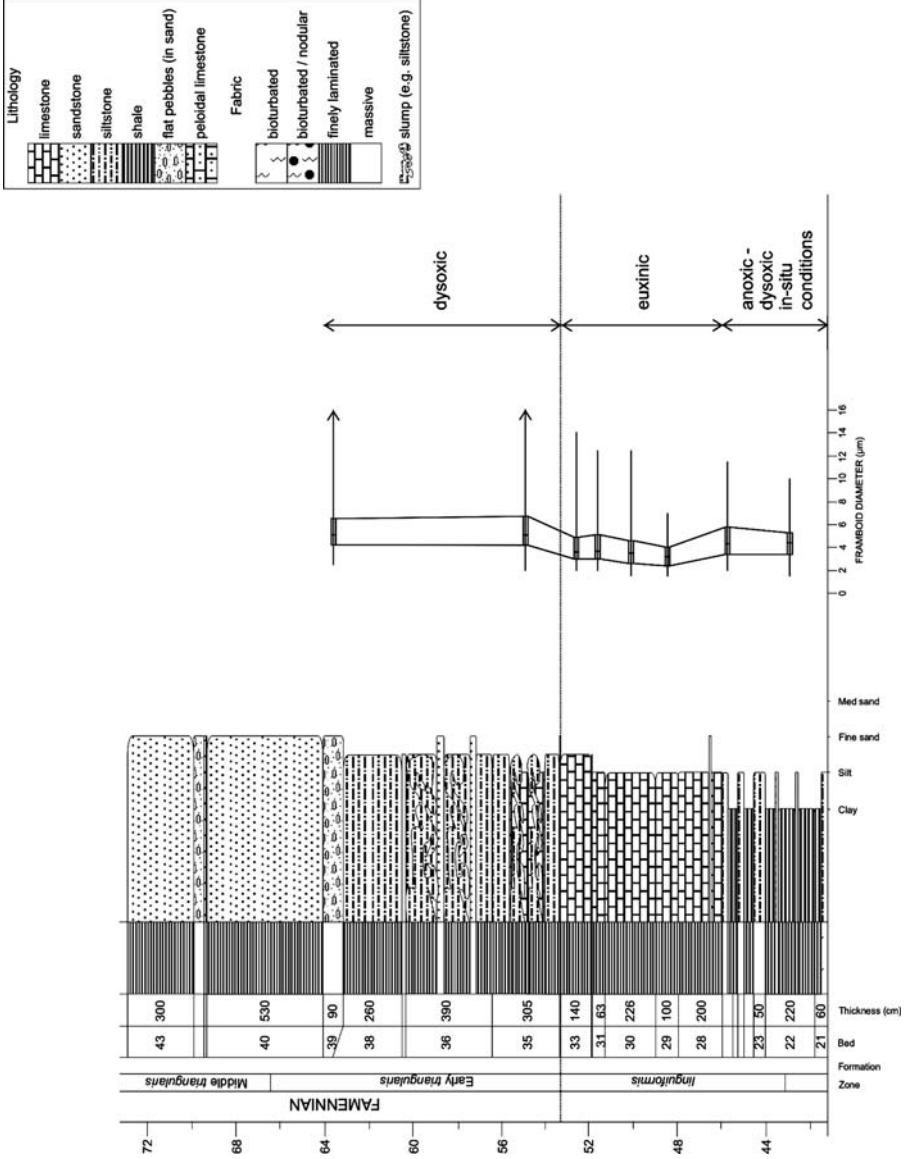
4.1.1. Lithological and faunal variations

Over 70 m of F-F sediments from the deep-water, intra-shelf Pilot Basin were studied (Fig. 5; see Appendix 1 for locality details). Sandberg et al. (1988, 1997) provide the most detailed account of the section, and have placed the F-F boundary precisely using conodont biostratigraphy. The base of the section is in the Early *rhenana* Zone, which contains the top-most part of the Guilmette Formation (beds 1–6). Above this, the remainder of the sequence comprises part of the lower member of the Pilot Shale, and continues up into the Middle *triangularis* Zone (beds 7–43).

The Guilmette Formation (beds 1–6) comprises well-bedded, thoroughly bioturbated, pale-grey micrites, with a rich fauna including corals, brachiopods, homoctenids, bivalves, goniatites, “spiny” ostracods, and trilobites. Micrite nodules and pyrite lumps are also present. The micrites are intercalated with a few brown calcareous siltstone and silty limestone horizons, which are also shown to be intensely bioturbated (Fig. 5).

The succeeding Pilot Shale (beds 7–43) is dominated by fine-grained, laminated shales, siltstones, and calcisiltites, with common pyrite blebs. These hemipelagic strata are interbedded with thin, siltstone turbidites, which contain shelf benthos and occasionally have bioturbated tops (e.g. bed 19, Fig. 5). Some beds (e.g. bed 15) have undergone slumping. Bed 18 records a change from quartz-rich calcisilt to a black, crinoidal wackestone, overlain again by quartz-rich siltstones. The F-F boundary lies at the top of bed 33, a finely laminated, brown, coarse calcisiltite. The basal Famennian, bed 34, is a graded conglomerate with many ooids and peloids and rare grapestones, floating in a calcisilt matrix. The early Famennian is characterised by an increased proportion of clastics, and a number of coarse siltstone and sandstone turbidites, which contain calcareous peloids and shelf benthos. There are also a number of additional conglomeratic debris-flow beds (Fig. 5).

Autochthonous benthic fauna in the Pilot Shale is scarce, but allochthonous fossils occur in the turbidites, and are dominated by a shelf fauna of crinoids and brachiopods. Rare, fragmented gastropods, and uniserial foraminifera are also observed in the Late



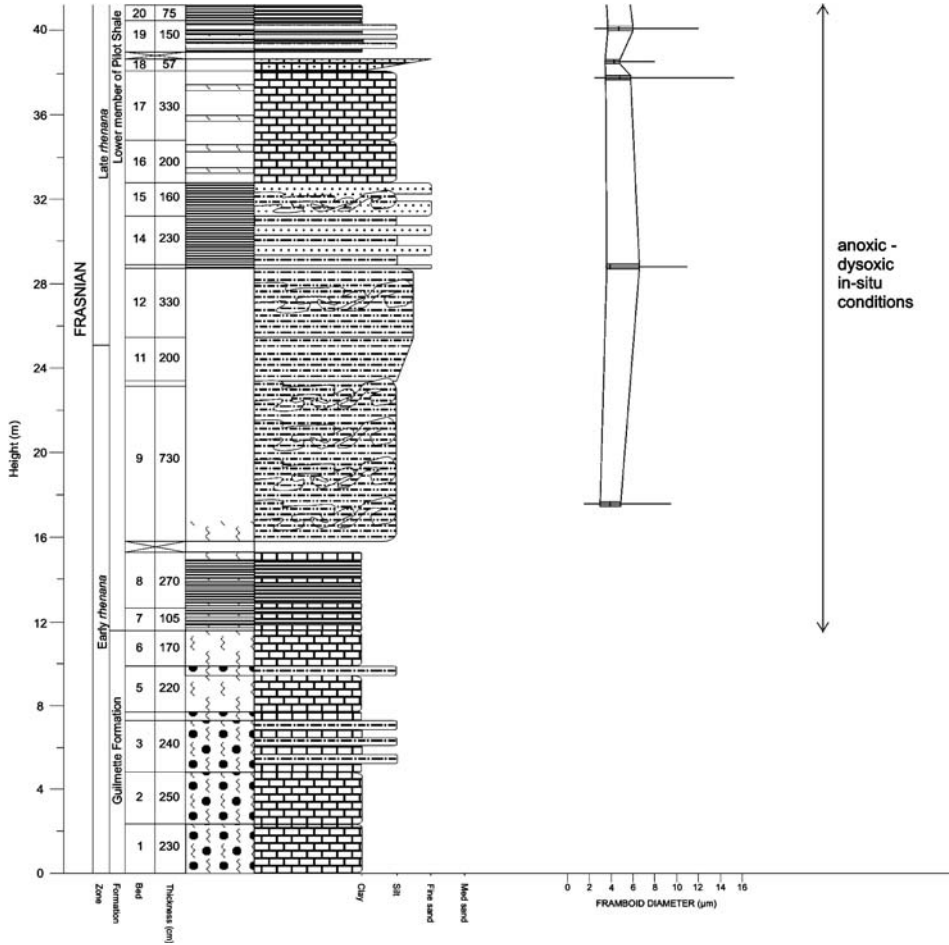


Figure 5. Log of Coyote Knolls section, including pyrite framboid “box and whisker” data (box shows 25th, 50th, and 75th percentile, with horizontal line representing minimum and maximum framboid diameter). Note that grade (e.g. clay) refers only to grain size, and not lithology, since this is a mixed clastic/and carbonate sequence. Conodont zonation based on Sandberg et al. (1997).

rhenana Zone. Homoctenids are occasionally observed within the Frasnian, but not above bed 28 in the *linguiformis* Zone. Within the topmost Frasnian, thin turbidites in beds 31 and 32 contain ostracods, crinoids, and abundant bioclasts. The early Famennian conglomerates contain crinoids, brachiopods, bryozoans, echinoderms, foraminifera, and other shell debris. Near the top of the section, in the Middle *triangularis* Zone, bed 41 contains abundant, small, prismatic-walled, circular fossils that are probably calcispheres. These are overgrown with a calcite cement.

4.1.2. Pyrite framboid analysis

Framboids are absent within the pale limestones of the Guilmette Formation, but in the overlying Pilot Shale, framboids become common (Fig. 6). Within the Early *rhenana* Zone, there are abundant, small framboids with a mean diameter of 4.3 μm (Fig. 6; Appendix B). In the Late *rhenana* Zone framboid mean diameter increases (ranging from 4.8 μm to 5.6 μm) and they are common in the finer-grained sediments. Bed 18, a black crinoidal wackestone, yielded only rare framboids in comparison to other beds. The overlying *linguiformis* Zone sediments also contain abundant framboids, although of smaller mean diameter (Fig. 6; Appendix B). Bed 29 is particularly rich in tiny framboids with a very small mean diameter of only 3.7 μm . In the Early *triangularis* Zone the framboid populations become less abundant and distinctly larger, with diameters up to 23 μm .

4.1.3. Depositional style and oxygenation history

Pyrite framboid, faunal, and lithological data all suggest that the Guilmette Formation was deposited in a well-oxygenated, shelf environment. The overlying Pilot Shale records a major deepening in the Early *rhenana* Zone (termed the *semichatovae* transgression, Sandberg et al., 2002), and a distinct change in environmental conditions. The finely laminated sediments, common turbidites, and slumped horizons indicate a basinal or distal base-of-slope environment. The lamination and common framboids within the calcisiltites suggest that oxygen-poor conditions prevailed with an anoxic seafloor developed throughout the Early to Late *rhenana* zones. The post-event bioturbation following turbidity flows suggests the turbidites are likely to have been sourced from the better-oxygenated shelf, from where they transported a living infauna that was able to briefly colonise and bioturbate the seabed, as is observed in some modern dysoxic basins (Follmi and Grimm, 1990). Not all of the turbidity flows caused oxygenation events, however, as bioturbation is rare in the upper part of the Late *rhenana* to *linguiformis* zones. This may reflect deteriorating oxygen levels on the shelf, although allochthonous shelf benthos remains present during the Late *rhenana* Zone. Alternatively, an intensely anoxic lower water column at this time may have been more immune to transient reoxygenation events.

The upper part of the Late *rhenana* Zone records a lithological change to more persistent and darker shales, with a corresponding decrease in framboid diameter, indicative of a decrease in benthic oxygen levels within the basin (Fig. 6). Pyrite framboid and lithological evidence suggest further deterioration in oxygen levels by the middle part of the *linguiformis* Zone, as fine lamination becomes persistent and the mean framboid diameter drops to 3.7 μm . Truly euxinic conditions probably developed at this time, and continued up to the F-F boundary. This is the level of the Upper Kellwasser Horizon in Europe. A

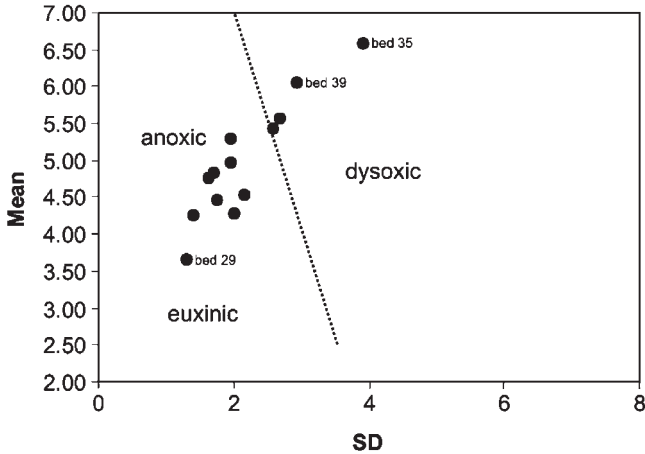


Figure 6. Mean frambooid diameter (microns) vs. standard deviation plot for pyrite frambooids at Coyote Knolls. Note that bed 29 (linguiformis Zone) plots as the most intensely anoxic bed, and that by beds 35 and 39 (Famennian), the frambooid distribution is characteristic of dysoxic conditions.

small amount of allochthonous benthic shelf fauna is observed, even within this level, indicating that anoxia probably did not develop in the sediment source area.

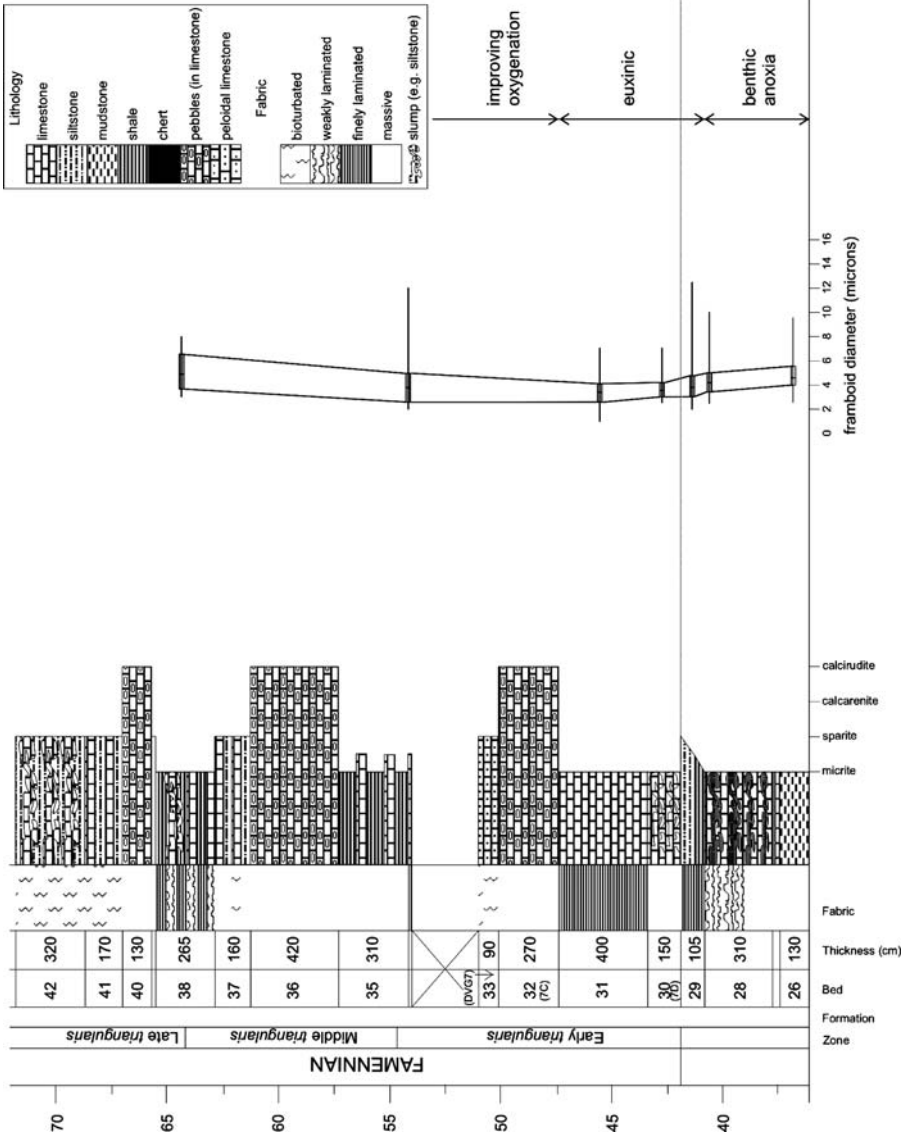
The basal Famennian records an improvement in oxygenation levels, with the frambooid distribution of bed 35 suggestive of a dysoxic setting. There is also the appearance of high-energy event beds, probably debris flows, that brought coarser material to the base-of-slope. Despite this improvement, the majority of the beds in the Early *triangularis* Zone remain finely laminated. Interestingly, allochthonous fauna becomes more abundant in the basal Famennian, with crinoids and brachiopods dominating, suggesting normal oxygen levels on the shelf.

4.2. Devils Gate

4.2.1. Lithological and faunal variations

This highly accessible section has been intensively studied (Sandberg and Poole, 1977; Sandberg et al., 1988, 1989, 1997, 2003; Casier et al., 1996; Morrow, 2000; Joachimski et al., 2002). It is regarded as one of the most important F–F reference sections (Sandberg et al., 1988, 2002), and the F–F boundary is well constrained by conodont dating. The sequence is a composite of three closely spaced sections (Fig. 7). In total a sequence of over 70 m in thickness, comprising 42 beds, has been investigated here.

This expanded sequence belongs to the upper member of the Devils Gate Limestone Formation (Fig. 7) and it ranges in age from the lower part of the Early *rhenana* Zone up to the Late *triangularis* Zone (Fig. 7). The base of the logged sequence corresponds to the “*semichatovae* transgression” (Sandberg et al., 1997, 2002, 2003) and the base of transgressive-regressive cycle II d of Johnson et al. (1985). This is manifest as a transition from



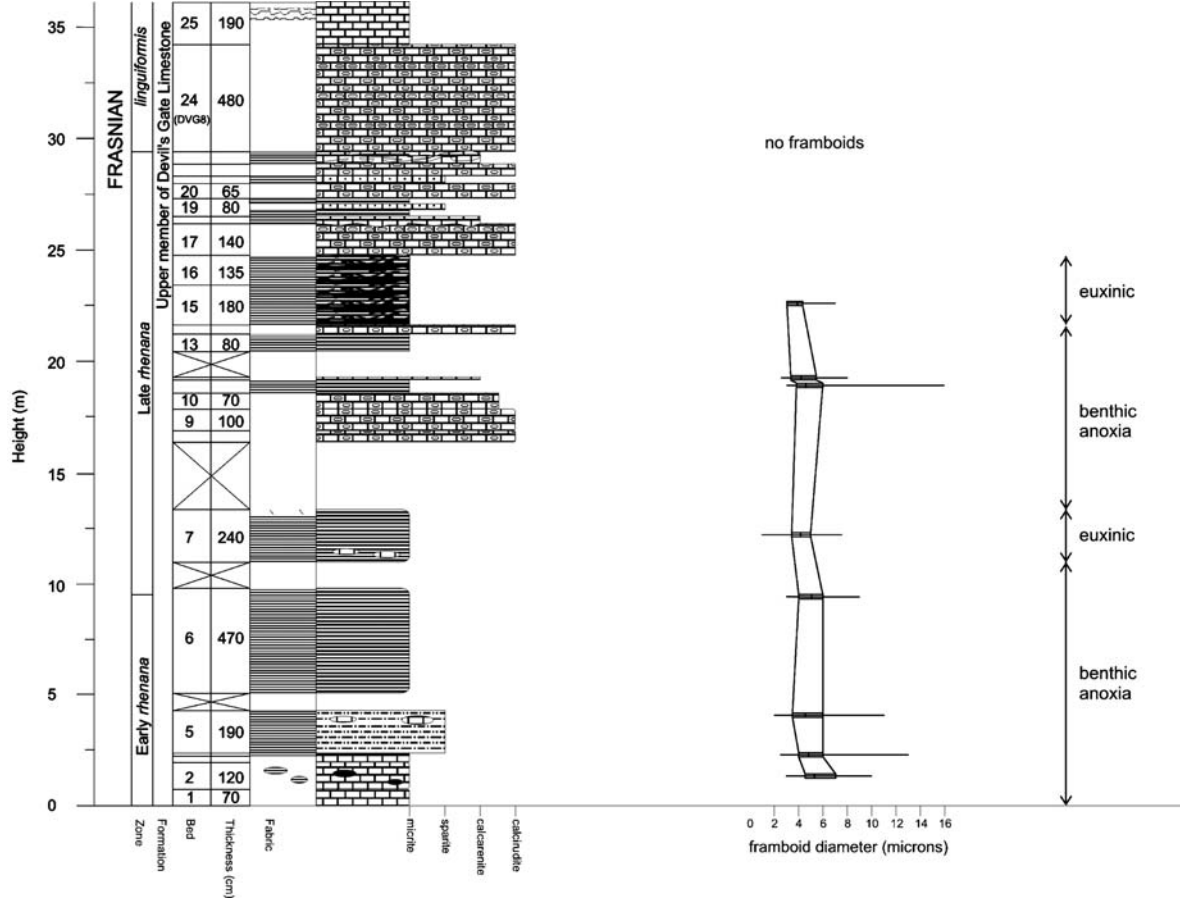


Figure 7. Log of Devils Gate section including pyrite framboid “box and whisker” data. Sample numbers from Sandberg et al. (1988) are given in brackets in bed column, where appropriate. Conodont zonation based on Sandberg et al. (1988).

medium-grey, massive micrites (beds 1–3) to organic-rich, dark, finely laminated radiolarian chert (bed 4), finely laminated siltstone (bed 5), and finely laminated, calcareous shale (bed 6).

Hemipelagic sedimentation during the Late *rhenana* to *triangularis* zones (beds 7–42) comprises cherts, silty shales, micrites, and calcareous siltstones, many of which are finely laminated. These often display slumping and soft sediment deformation. The fine-grained sediments are frequently interbedded with thick beds of limestone breccia and conglomerate, which are usually clast supported and lack clast orientation. The clasts include peloidal limestones, large flat pebbles, and chert pebbles (e.g. beds 8–9, 14, 17, 20, 22, 24, 32, 36, and 40). A number of calcarenite turbidites are also present. During the upper part of the *linguiformis* Zone, there was a brief pause of this allodapic deposition (bed 24 is the highest Frasnian sediment-gravity flow), allowing persistent hemipelagic sedimentation across the F-F boundary. The rocks at this level comprise massive to weakly laminated mudstones and shales. The F-F boundary, defined by conodonts, is placed at the top of bed 29, a badly weathered, finely laminated, silty shale, which coarsens upwards into siltstone (Sandberg et al., 1988; Fig. 7). The basal Famennian is characterised by turbidites, interbedded with siltstones and shales. There are numerous thick conglomerates in the Early and Middle *triangularis* zones, which again are interbedded with siltstones. The topmost part of the sequence (Late *triangularis* Zone) becomes dominated by a “ribbon facies” of interbedded micritic limestones and siltstones on a scale of a few centimetres.

The non-conodont fauna in the Devils Gate section is varied, but not abundant, and is mostly restricted to allochthonous shelf fauna within the turbidites and coarser beds (Fig. 7). Other than abundant conodonts, the Early *rhenana* Zone hemipelagic sediments contain only occasional calcispheres, and radiolarians within some chert beds. Bioturbation is absent except for that seen within silty, sparry concretions in bed 5, where the fine lamination has been partly disrupted by burrowing. In the Late *rhenana* Zone the thick calcirudites contain a rich shelf fauna of crinoids, silicified rugose corals, *Syringopora*, stromatoporoids, echinoderm fragments, gastropods, brachiopods, ostracods, several species of foraminifera, calcareous algae (possibly gymnocodiaceans), and calcispheres. In contrast, background sediments generally remain finely laminated, and without fossils. Bed 24 marks the base of the *linguiformis* Zone, and contains a rich shelf fauna similar to that of the beds below. In addition, Sandberg et al. (1988) recorded common *Iowatrypa* and *Tabulophyllum* within this bed. Indeed bed 24 marks the last occurrence of both these genera (Fig. 7). The *linguiformis* Zone hemipelagic-style sediments (beds 25–29) contain small, unidentified bioclasts, and calcispheres. At this level the beds are massive or weakly bioturbated although the topmost Frasnian, bed 29, records a distinct change to unfossiliferous, finely laminated silty shales, from the more massive or weakly bioturbated beds beneath (Fig. 7).

The basal Famennian turbidites contain a fauna including brachiopods, (probably *Leiorhynchus*) and abundant calcispheres. These are interbedded with unfossiliferous hemipelagic sediments. The conglomerates in the Early and Middle *triangularis* zones contain a diverse, allochthonous fauna of solitary rugose corals, foraminifera (belonging to different taxa to those seen in the Frasnian strata), crinoids, brachiopods, ostracods, calcified cyanobacteria, large orthocone nautiloids, and calcispheres. The intervening sediments are mostly massive or bioturbated. The Late *triangularis* Zone is generally bioturbated and contains thin-shelled brachiopods, ostracods, calcispheres, and fusulinid foraminifera (Fig. 7).

In a study of the ostracods from F-F boundary strata at the Devils Gate section, Casier and Lethiers (1998) noted the presence of an abundant, but allochthonous, Frasnian and Famennian fauna. Seventy ostracod species were identified within the Frasnian, belonging to an association typical of well-oxygenated, marine conditions (Casier and Lethiers, 1998). This undoubtedly records conditions in the source area of the allodapic limestones and not at the depositional site. Of these species, 16 pass through the F-F boundary, indicating a severe extinction rate in excess of 75%.

4.2.2. Pyrite framboid analysis

SEM analysis of the fine-grained, hemipelagic strata of the Early *rhenana* to Late *triangularis* zones reveals that framboidal pyrite is common throughout much of the Devils Gate sequence. In the Early *rhenana* Zone, bed 2 contains uncommon framboids with a relatively large mean diameter (Fig. 8; Appendix B). Above this bed, the silty shales of beds 4–7 (the record of the *semichatovae* transgression), contain abundant, small framboids. The framboids become even smaller at the base of the Late *rhenana* Zone, in a finely laminated, black, silty shale. Above this (bed 11) there is an increase in mean diameter and during the middle part of the Late *rhenana* Zone (beds 12 and 15) framboids are uncommon and somewhat smaller. Framboids were not found in samples from the upper part of the Late *rhenana* Zone.

Framboids become common once again in the upper part of the *linguiformis* Zone. In the topmost Frasnian, the middle part of bed 29 contains abundant, small framboids, which record a decrease in mean diameter to only 4.4 μm . The Early *triangularis* Zone hemipelagic sediments also contain common, small framboids with very similar mean diameters, but by the Late *triangularis* Zone, only rare, large framboids are present (Fig. 8; Appendix B).

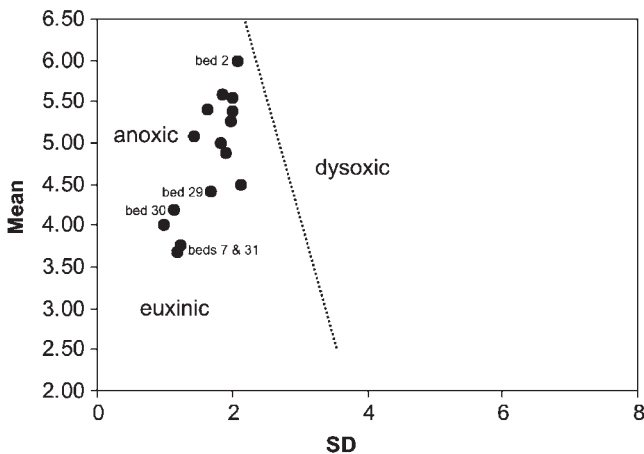


Figure 8. Mean frambooid diameter (microns) vs. standard deviation plot for pyrite framboids at Devils Gate. Note that the sequence as a whole plots within the anoxic/euxinic fields, with bed 7 (basal Late *rhenana* Zone) and beds 29–31 (F-F boundary beds) plotting as the most intensely anoxic beds.

4.2.3. Depositional style and oxygenation history

The interbedding of fine-grained strata and thick, limestone breccias, conglomerates, and turbidites together with the common slumped horizons and soft sediment deformation is indicative of slope deposition at Devils Gate. As at Coyote Knolls, the material moving down-slope was sourced from an oxygenated area where a diverse shelly benthos thrived. However, the various gravity flows clearly came to rest in an anoxic setting as testified by the abundant framboids and fine lamination of the interbedded fine-grained strata. Peak intensity of anoxia (i.e. euxinic conditions), characterised by the smallest framboid populations, was encountered in the early to middle part of the Late *rhenana* Zone and the late part of the *linguiformis* Zone. The intervening interval is recorded by strata that are massive or bioturbated and lack pyrite. This suggests that oxygen levels at the depositional site increased slightly at this time, although they probably remained dysoxic, as some beds are laminated. The basal Famennian hemipelagic sediments (beds 30 and 31) also contain common framboids, with size distributions indicating that the latest Frasnian euxinic pulse continued into the Early *triangularis* Zone. However, the presence of rare, dysaerobic brachiopods in bed 30 (*Leiorhynchus*) suggests dysoxic interludes. Later in the *triangularis* Zone an increase of the size and a decline in abundance of framboids indicates an improvement in benthic oxygen levels. During the Late *triangularis* Zone, beds 41 and 42 record the return of weak bioturbation.

The fluctuating intensity of bottom water oxygen-restriction may reflect relative sea-level changes in the Devils Gate section. Thus, the onset of anoxia in the Early *rhenana* Zone may correlate with the *semichatovae* transgression (Event 8 of Sandberg et al. (1997) and Event 4 of Sandberg et al. (2002)). Improvement of benthic oxygenation in the Late *rhenana* to early *linguiformis* zones may reflect subsequent shallowing, although this was rapidly superseded by euxinic-style deposition and probably rapid deepening across the F-F boundary. After a relatively quiet period of deposition during the late *linguiformis* Zone, the early part of the Famennian is characterised by high-energy events. Bed 32 is a large debris flow, interpreted to be a tsunamite by Sandberg et al. (1988) because, unlike other debris flows at Devils Gate, it contains abundant clasts of nearshore carbonates and reworked Frasnian conodonts at its top. It is also markedly erosive at its base and locally erodes down to a level in the uppermost Frasnian strata (Sandberg et al., 2003; Morrow and Sandberg, 2003).

4.3. Northern Antelope Range

4.3.1. Lithological and faunal variations

This highly expanded, composite section (Fig. 3; Appendix A) has previously been studied by Johnson et al. (1980, 1996), Hose et al. (1982), Morrow (2000), Morrow and Sandberg (2003), and Sandberg et al. (2003). At the base of the studied section several metres of finely laminated cherts and shales occur, interbedded with thin beds of turbiditic calcarenites. This is the upper part of the lower tongue of the Woodruff Formation (beds 1–6, Late *rhenana* Zone) and the calcarenites are composed of well-sorted, well-rounded grains of peloids (Fig. 9). This material dominates the overlying Fenstermaker Wash Formation (beds 7–26, Late *rhenana* to Early *triangularis* zones), which consists of thick beds of massive, peloidal,

sandy calcarenites with significant quartz grain content. The peloids are strikingly well-sorted and rounded (Fig. 10). There is little lithological variation within the Fenstermaker Wash Formation until the *linguiformis* Zone, when the calcarenites become finer grained and have a markedly reduced quartz content (Morrow, 2000; Morrow and Sandberg, 2003). The lower Famennian (bed 22) is a distinctive calcirudite containing rounded, 5-cm-diameter pebbles of micrite, and silicified bioclasts. Above this, microsparites and peloidal calcarenites extend to the top of the section (Fig. 9).

Fauna in the Woodruff Formation is extremely sparse and limited to radiolarians, conodonts, and sponge spicules. The Fenstermaker Wash Formation is equally, poorly fossiliferous. Calcispheres are scattered throughout, although they are rare in the topmost Frasnian. Other fossils include silicified brachiopods and crinoids in beds 22–26, but generally the high degree of rounding and sorting of peloids suggests poor preservational conditions for fossils.

4.3.2. Pyrite framboid analysis

The cherty beds of the Woodruff Formation contain common framboids, with small mean diameters between 5–6 μm , but relatively large MFD values up to 25 μm (Fig. 9). No framboids are observed in the Fenstermaker Wash Formation although bed 20 of the *linguiformis* Zone contains common pyrite blebs, in contrast to the surrounding beds that lack pyrite.

4.3.3. Depositional style and oxygenation history

The finely laminated cherts and shales of the Woodruff Formation indicate a deep-water environment and the presence of calcareous turbidites suggests a base-of-slope depositional environment. The considerable bed thickness and lack of grading displayed by the calcarenites of the succeeding Fenstermaker Wash suggests that they are not typical turbidites. Instead, they may record high-concentration turbidity flows from close to source or even grain flows. Morrow (2000) and Sandberg et al. (2003) record deep-water conodonts within the Fenstermaker Wash Formation, in keeping with a slope interpretation. However, they interpreted the sediments to have formed on a shallow-water carbonate bank setting in which case the sediment-gravity flows must have entrained conodonts while they flowed down-slope, or alternatively the conodonts accumulated in the slope setting between gravity-flow events.

The absence of hemipelagic sediments in the Fenstermaker Wash Formation renders the reconstruction of oxygen levels at the depositional site extremely difficult. However, the cherts and shales of the underlying Woodruff Formation, within the Late *rhenana* Zone, are finely laminated and exhibit pyrite framboids with a size distribution characteristic of an anoxic environment. The high MFD in these beds suggests that bottom waters were occasionally dysoxic thereby allowing large framboids to grow within the surface layers of the sediment. The appearance of pyrite blebs in bed 20, in the later part of the *linguiformis* Zone, probably reflects a subtle decrease in oxygen levels although assessing any redox variations in such rapidly deposited, allochthonous carbonates is problematic. The scarcity of fossils in the Fenstermaker Wash Formation reflects a taphonomic control (i.e. a high energy source area inimical to the preservation of fossils) and does not allow inferences about oxygen levels at the depositional site. Allochthonous benthos is not recorded during the Frasnian but becomes common in the early Famennian. This may again be preservation controlled, but also might reflect an improvement in oxygen levels on the shelf source area at this time.

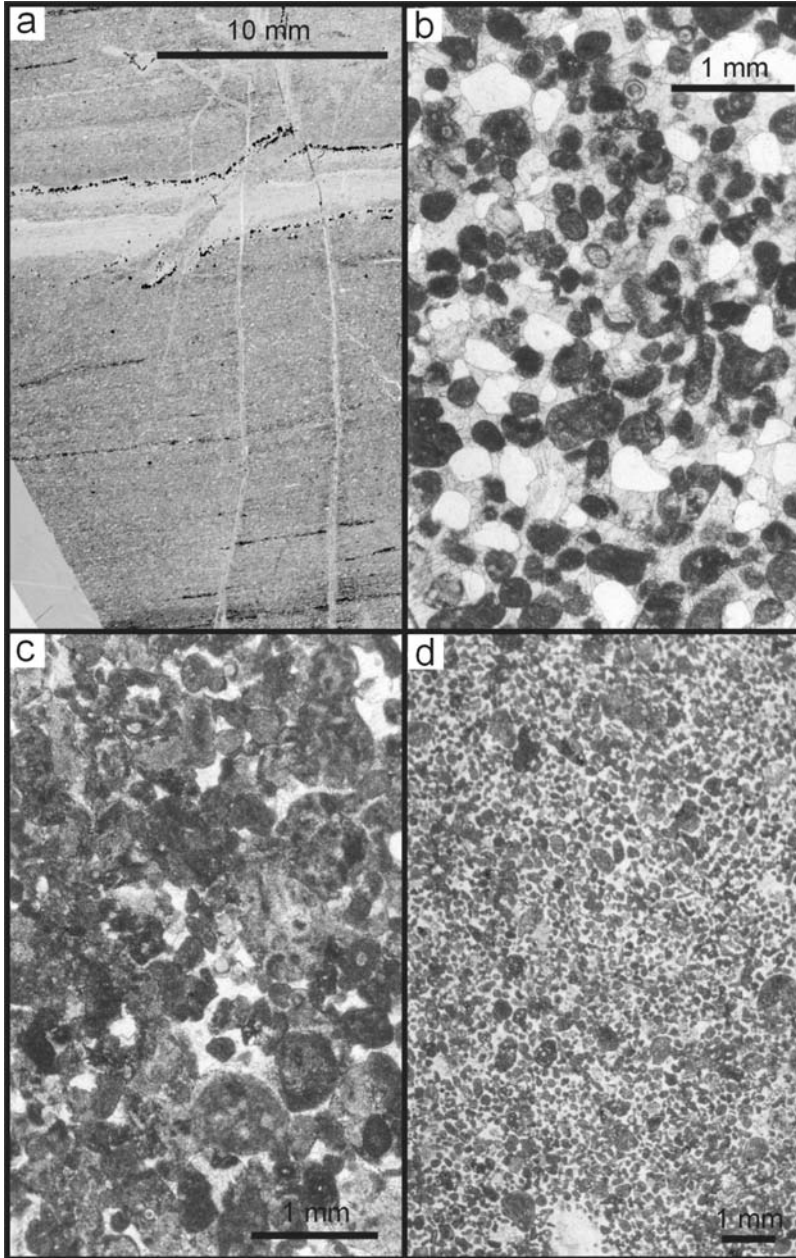


Figure 10. Photomicrograph of Northern Antelope Range rocks: (a) Lower part of bed 4 (Late *rhenana* Zone), finely laminated, pyritic calcareous shale of the Woodruff Formation; (b) Bed 8 (Late *rhenana* Zone), well-rounded, peloidal calcarenite, consisting of approximately 60% peloids and 40% quartz grains; (c) Bed 20 (*linguiformis* Zone), fine-grained calcarenite with notably reduced clastic content; and (d) Lower Famennian bed 23, peloidal microsparite.

The dramatic facies change between the two formations is interpreted to be the result of proto-Antler forebulge migration, which caused large amounts of sediment to be washed down-slope (Sandberg et al., 2003). The unusual facies of peloidal calcarenites (see Fig. 13), supplemented in the boundary beds by common, abraded bioclasts are similar to those described from the Famennian-age Palliser Formation of western Canada (Peterhaensel and Pratt, 2001). Although the source is unclear, these authors argued that excess nutrients in the ocean led to unusually high levels of microendolithic bioerosion of the skeletal grains deposited on the carbonate platform. Consequently, bioclasts (predominantly crinoids in the Canadian example) were intensely bored to form micritic peloids, and cortoids. The destruction of bioclasts clearly would mask the diversity and abundance of shelf benthos.

4.4. *Tempiute Mountain*

4.4.1. *Lithological and faunal variations*

No specimens of *Palmatolepis linguiformis* have been found in this 20 m-thick mountainside section (Fig. 11); however, late evolutionary variants of *rhenana* Zone conodonts are present, suggesting that the *linguiformis* Zone is present (Morrow, 2000; Morrow, pers. comm. 2002). The studied section begins in this probable *linguiformis* Zone strata and continues up into the Early *crepida* Zone, and belongs entirely to the Devils Gate Limestone. Here, the Devils Gate consists of thin-bedded, laminated to bioturbated micrites, microsparites, and calcisiltites (Fig. 11). Interbedded with these sediments are common, massive calcisiltite, calcarenite, and sandstone turbidite beds of varying composition, which show common syndepositional deformation (Morrow and Sandberg, 2003). The upper Frasnian turbidites are carbonate dominated, whereas those in the lower Famennian are mostly sandstones. The F-F boundary has not been precisely constrained, but is thought to lie within a short, unexposed interval between beds 8 and 9. The lower Famennian strata consist of sandstone turbidites that contain flat pebbles of limestone. At the top of the section, beds 14 and 15 are laminated, pyritic, medium-to-dark-grey micrites (Fig. 11).

Fauna in the main Tempiute Mountain boundary section is sparse. Samples recovered from the *punctata* to *jamieae* Zone strata below the study section shown in Fig. 11 contain poorly preserved tentaculitoids and ostracods. Much of the fauna is contained within the turbidite beds, and includes crinoids, tentaculitoids (in bed 4), ostracods, bivalves, conodonts, and calcispheres. No fossils, other than conodonts, were observed in the *triangularis* Zone, but in the *crepida* Zone, bed 15 contains abundant siliceous sponge spicules, calcispheres, and rare brachiopod fragments.

4.4.2. *Pyrite framboid analysis*

Most samples from Tempiute Mountain do not yield framboids. However, the fine-grained sediments occasionally reveal very small numbers of framboids, often with small diameters (Fig. 11; Appendix B), in particular in the upper part of the *linguiformis* Zone. Much of the sequence around the boundary contains pyrite blebs, but only bed 14, in the Late *triangularis* Zone, contains common framboids, with a mean diameter of 6.8 μm (see Fig. 15).

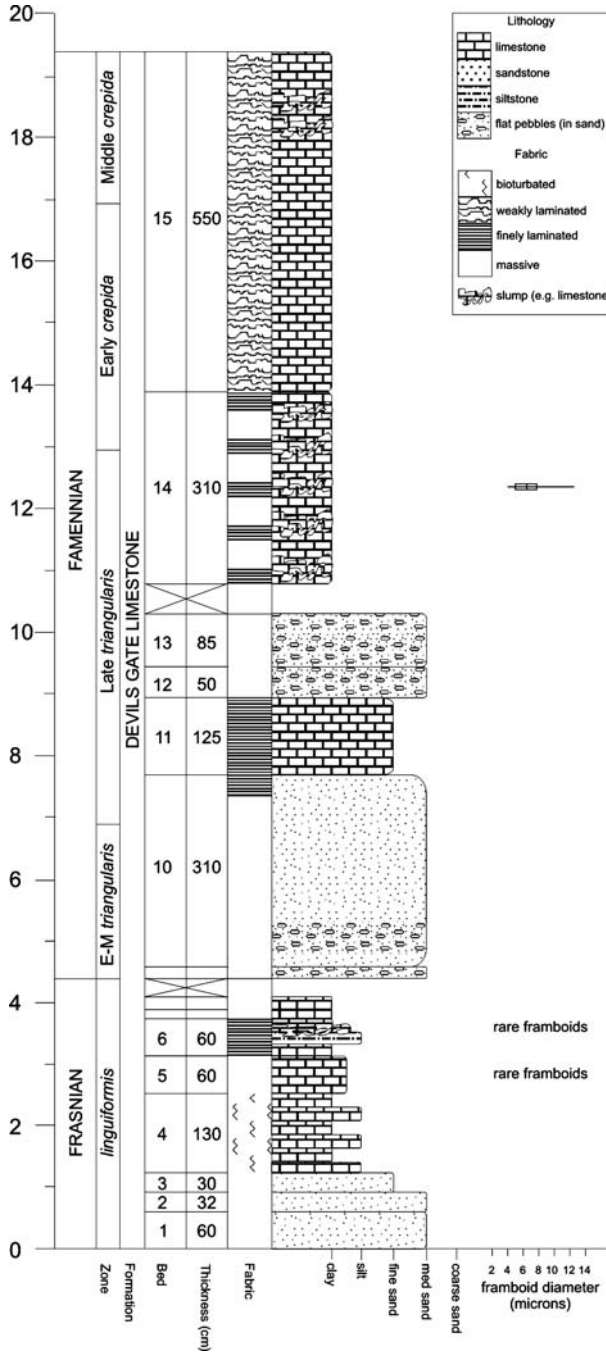


Figure 11. Log of Tempiute Mountain section including pyrite framboid “box and whisker” datum. Note that grade (e.g. clay) refers only to grain size, and not lithology, since this is a mixed clastic/and carbonate sequence. Conodont zonation based on Morrow (2000).

4.4.3. Depositional style and oxygenation history

Turbidites and background hemipelagic strata typical of a base-of-slope or basin floor depositional setting dominate this section. However, elsewhere in the F-F stratigraphy (*linguiformis* to Early *crepida* zones) slump folding is common indicating a slope setting (Morrow, 2000; Morrow and Sandberg, 2003). There is a noticeable change in sediment source across the F-F boundary from carbonate-sourced to clastic-sourced turbidity flows.

Pyrite framboids provide tentative evidence for anoxia at Tempiute Mountain but their rarity is rather enigmatic. Most of the turbidite beds are not framboidal, and contain a benthic fauna sourced from a shelf. The lack of an in-situ benthic fauna and presence of lamination suggests oxygen-depleted benthic conditions. However, conditions were not persistently anoxic, resulting in occasional bioturbation. Bed 6 exhibits persistent, fine laminations, and those framboids that have been found are very small, suggesting that euxinic conditions may have developed during the late part of the *linguiformis* Zone.

As in other sections, the early Famennian witnessed the appearance of abundant intraclasts, most notably of the “flat pebble” variety, at Tempiute Mountain. A similar appearance of flat-pebble conglomerates is also seen in equatorial sections in the immediate aftermath of the end-Permian mass extinction (Wignall and Twitchett, 1999). They record the early lithification of thin beds of carbonate that have not been bioturbated. The lack of such burrowing may be a signal of oxygen-restriction in the shallower-water source area of such intraclasts.

Finely laminated sediments and relatively small framboids in the Late *triangularis* to Early *crepida* zones provide clear evidence for anoxia, although the presence of sponge spicules in the *crepida* Zone suggests that benthic conditions improved to at least dysoxic levels allowing this benthic fauna to develop. The F-F boundary was not seen at Tempiute Mountain and it is not possible to conclusively state whether an anoxic event occurred at the boundary. However, lithological, faunal, and pyrite analyses suggest that conditions were probably oxygen-poor throughout the F-F interval.

4.5. Whiterock Canyon

4.5.1. Lithological and faunal variations

This canyon section from near Horse Heaven Mountain, Nevada, comprises 20 m of section divided into 13 beds. Deposited in the Woodruff Basin, the section spans the Early *rhenana* to Late *triangularis* zones, and is entirely developed within the Woodruff Formation (Bratton et al., 1999; Morrow, 2000; Morrow and Sandberg, 2003). This comprises dark, finely laminated cherts and shales, interbedded with thin siltstones, some of which are calcareous (Fig. 12). Several of the *linguiformis* Zone beds are notably organic-rich. There is evidence for minor slumping in bed 3, but the majority of beds are undisturbed. The topmost Frasnian level (bed 6) is a finely laminated dark-grey to black, silty, organic-rich chert with common pyrite, that becomes siltier in its upper part. The directly overlying Famennian beds consist of siltstone rather than chert. The silt occurs as thin, graded laminae.

Bioturbation is absent in the Whiterock Canyon section and fossils are sparse (Fig. 12), other than abundant radiolarians in the Frasnian, especially in the topmost *linguiformis* Zone (bed 6). No fossils other than conodonts are found in the Famennian.

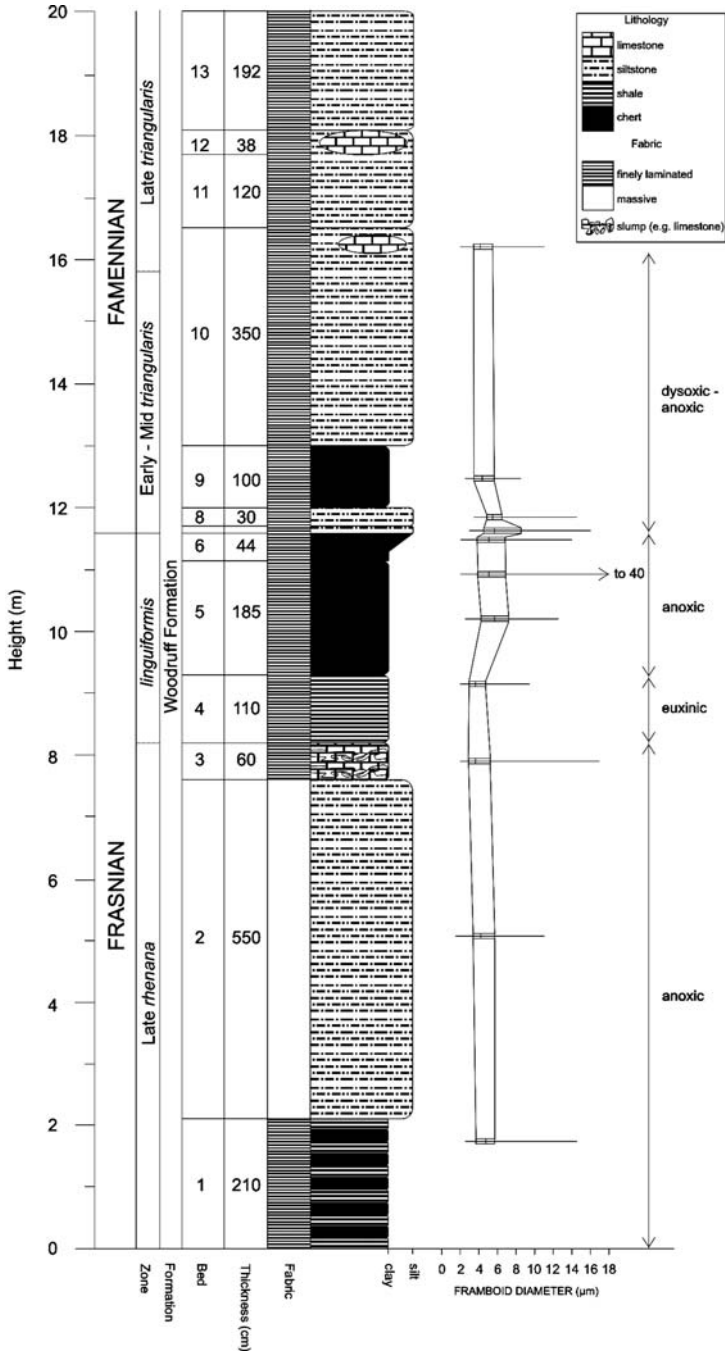


Figure 12. Log of Whiterock Canyon section, including pyrite framboid “box and whisker” data. Conodont zonation from Morrow (2000).

4.5.2. Pyrite framboid analysis

Polished blocks examined under the SEM reveal that almost the entire Whiterock Canyon sequence contains framboidal pyrite (Fig. 13; Appendix B). Within the Late *rhenana* Zone, beds 1 and 2 contain common framboids with consistent, small mean diameters. Bed 3 records a decrease in mean framboid diameter, and there is a further decrease in the *linguiformis* Zone (bed 4). In the middle and upper part of the *linguiformis* Zone, beds 5 and 6 contain abundant framboids, which record a small rise in mean diameter. The top of bed 5 (upper *linguiformis* Zone) has a much larger maximum framboid diameter of 40 μm (Fig. 13; Appendix B). By the topmost Frasnian, bed 6, framboids are again abundant and record a decrease in mean diameter, although they are slightly larger than those in the lower part of the sequence. There is an increase in mean framboid diameter in the basal Famennian, coincidental with the increased input of detrital silts within turbidites. This may in part be due to winnowing and reworking of framboids in the silt turbidites, resulting in the smallest framboid fraction being lost. Beds 7 and 8 contain less-abundant framboids with an increased mean diameter (Fig. 13; Appendix B). During the Middle *triangularis* Zone, framboids again become abundant, and record another drop in mean diameter to small sizes.

4.5.3. Depositional style and oxygenation history

The fine-grained nature of the sediment suggests deposition within a low energy, deep-water setting, although the thin, graded siltstones of the Famennian may record the distal-most development of a prograding turbidite succession. Sedimentation rates were clearly substantially lower than those seen in the more proximal slope sections to the east (Fig. 3).

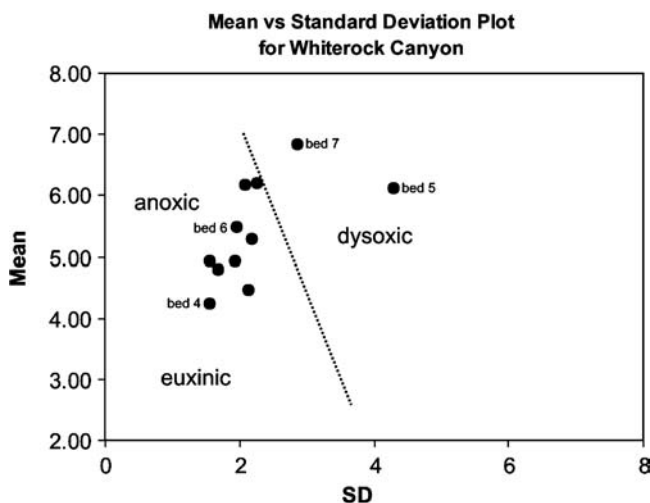


Figure 13. Mean framboid diameter (microns) vs. standard deviation plot for pyrite framboids at Whiterock Canyon. Note that most beds plot within the anoxic field, with beds 5 (*linguiformis* Zone) and 7 (Early *triangularis* Zone) plotting in the dysoxic field.

Pyrite framboid data and the fine laminae suggest that depositional conditions were persistently anoxic in this deep-water setting within the Woodruff Basin. However, there was subtle variation on this theme with small sizes and low size variability of early *linguiformis* Zone framboids indicating euxinic conditions. In the higher parts of the *linguiformis* Zone, the larger mean framboid diameter suggests conditions improved slightly to anoxic-dysoxic levels.

In the Early *triangularis* Zone, beds 7 and 8 both record a higher mean framboid diameter, characteristic of dysoxic conditions. These beds contain a succession of thin, distal turbidites, which might have led to a brief improvement in benthic oxygen levels, or alternatively modification (winnowing) of the framboid populations during transport. However, by the Middle *triangularis* Zone, the framboid distribution indicates that conditions again deteriorated to anoxic levels that prevailed to the top of the section.

4.6. Warm Springs

4.6.1. Lithological and faunal variations

The 15-m-thick Warm Springs section, which is developed within the Woodruff Formation (Sandberg et al., 1997), has been divided into eight beds and spans the Early *rhenana* Zone to earliest Famennian. The base of the section comprises black, finely laminated cherts, and light-grey, finely laminated, pyritic siltstones, interbedded on a 5 mm–5 cm scale (Fig. 14). There is also a thin chert breccia consisting of chert clasts within a chert matrix that may be the product of tectonic cataclasis. The Late *rhenana* to *linguiformis* zones expose weakly bioturbated, pyritic, red, calcareous siltstone, with lenticular lenses of black, laminated chert. Part of bed 6 has undergone considerable deformation, possibly during slumping. Bed 7 comprises laminated, pyritic, calcareous siltstones, which weather red but are dark-grey when fresh. The F-F boundary has not been precisely placed using conodonts, but is constrained to within bed 7 (Sandberg et al., 1997; Morrow, pers. comm. 2002). Thus, the topmost Frasnian records a distinct lithological change from bioturbated to laminated silts. The early Famennian section shows intense tectonic deformation and consists of black cherts (Fig. 14).

As at Whiterock Canyon, fossils are extremely rare in the Warm Springs section apart from the abundant radiolarians in the chert beds, and microfaunas recovered from rare carbonate concretions. Also similar is the disappearance of radiolaria towards the F-F boundary, although in this section they return in the Famennian.

4.6.2. Pyrite framboid analysis

Warm Springs samples contain very rare pyrite framboids except around the F-F boundary where they become more common (Fig. 14). Very rare, but quite small framboids occur in the sediments of the Early *rhenana* and Late *rhenana* zones (Appendix B).

4.6.3. Depositional style and oxygenation history

This is a condensed section of cherts and fine siltstones in which pelagic and hemipelagic deposition dominated, although there is possible evidence for minor slumping during the

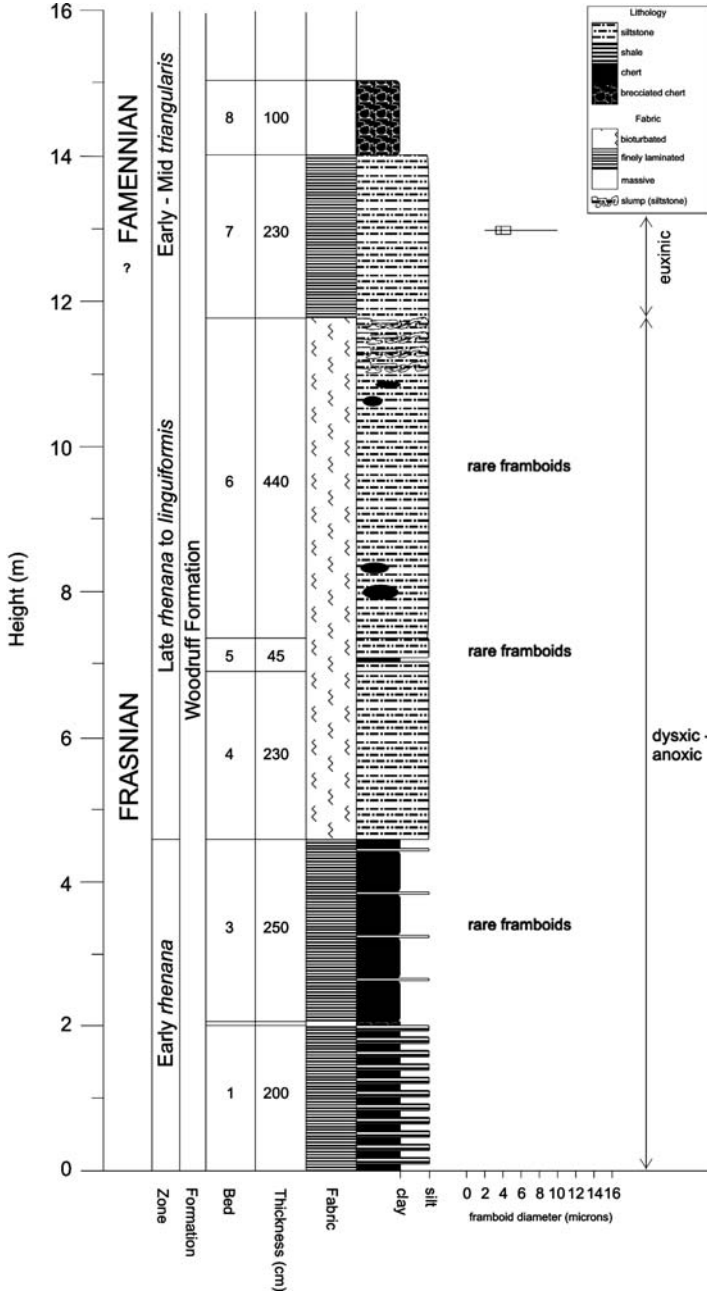


Figure 14. Log of Warm Springs section including pyrite framboid “box and whisker” data. Conodont zonation from Sandberg et al. (1997).

linguiformis Zone. A basin floor setting appears appropriate, although Sandberg et al. (1997) suggested a “transitional” location between lower slope and basin based on the occurrence of olistoliths (not seen in this section) derived from the carbonate platform to the east. It is of course possible for olistoliths to travel considerable distances along a basin floor. Whatever the precise location within the basin, Warm Springs is clearly a deep-water distal section.

Oxygen-restricted deposition clearly dominated deposition at Warm Springs section although the higher parts of the Late *rhenana* Zone display small burrows (Ichnofabric Index 2–3, Droser and Bottjer, 1986) and a decline in framboidal pyrite abundance indicating improvement of benthic oxygen levels. The most intensely anoxic conditions are recorded in the F-F boundary and lowest Famennian strata where small-diameter framboids are abundant.

5. Discussion

5.1. Summary of oxygenation history

To the east of the proto-Antler forebulge, the slope and basin floor sections of the relatively shallow intra-shelf, Pilot basin (e.g. Devils Gate and Coyote Knolls) records persistent anoxic conditions during most of the studied F-F interval, probably due to the semi-restricted nature of deposition in this intracontinental basin (Figs. 15 and 16). Compared with the Devils Gate section, the intensity of anoxia is generally greater and more persistent in the Coyote Knolls section. This probably reflects its deeper-water location. Thus, persistent euxinic conditions are developed throughout the late *rhenana* to end-*linguiformis* interval at Coyote Knolls while euxinic conditions at Devils Gate began later (late *linguiformis* Zone) and persisted a little longer (Early *triangularis* Zone).

Anoxic sedimentation on the slope of the Pilot basin was frequently interrupted by turbidites and debris flows that contain a diverse shelf fauna, indicating oxygenated conditions in the source area which was probably the crest of the proto-Antler forebulge. Casier

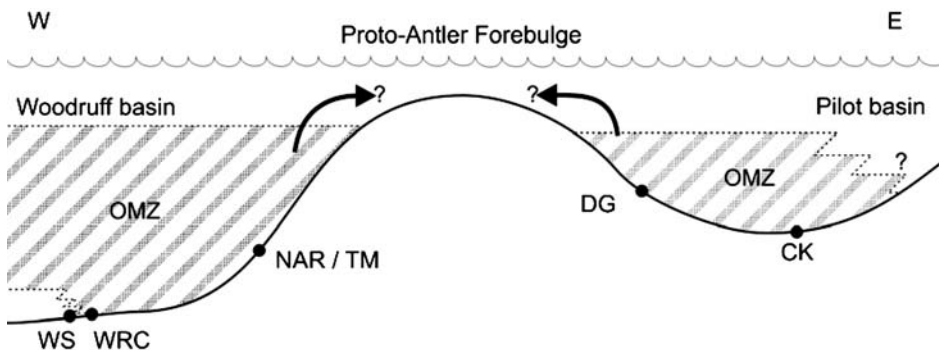


Figure 15. Schematic cross-section showing estimated palaeogeographic positions of Great Basin Frasnian-Famennian sections, and inferred oxygen minimum zone (OMZ) during the latest Frasnian (WRC = Whiterock Canyon; WS = Warm Springs; NAR = Northern Antelope Range; DG = Devils Gate; TM = Tempiute Mountain; CK = Coyote Knolls). Arrows indicate potential spilling of anoxic waters onto shallow shelf areas during latest Frasnian.

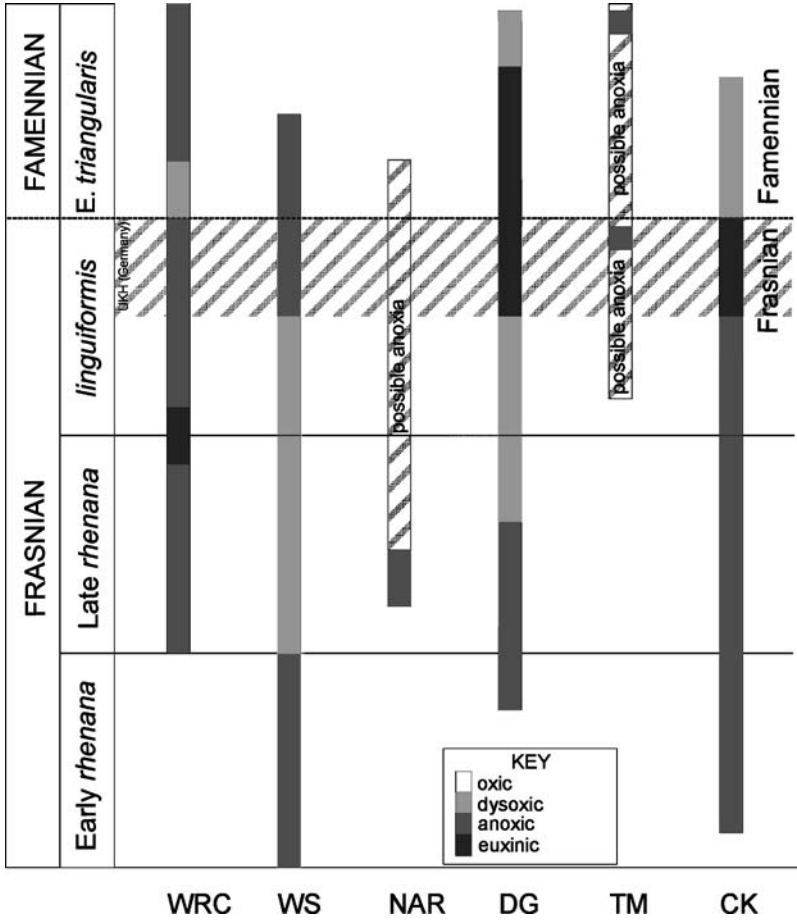


Figure 16. Timing of development of oxygen-poor conditions in the Great Basin (section abbreviations as in Fig. 1). Note that true palaeo-oxygenation conditions across the F-F boundary in NAR and TM sections are probably masked by turbidite events. The hachured shaded band relates to the development of anoxia in the Devils Gate and Coyote Knolls sections and is contemporaneous with the Upper Kellwasser Horizon in Germany.

and Lethiers (1998) identified a diverse ostracod assemblage within the Frasnian at Devils Gate indicative of a well-oxygenated environment but no assemblage characteristic of oxygen-depleted conditions has been identified close to the boundary. However, the ostracods are allochthonous, because they are found within turbidites and debris flow beds derived from the shelf, and these data lend further support to the suggestion that the shelf remained oxygenated. The ostracod evidence does not, however, preclude anoxic conditions developing at the depositional site.

To the west of the Pilot Basin and the adjacent proto-Antler forebulge, the eastern slopes of the Woodruff Basin were dominated by rapid deposition of allochthonous strata (e.g. Northern Antelope Range and Tempiute Mountain). These preserve a poor record of palaeo-oxygenation levels. However, interbedded hemipelagic sediments of the Late rhenana and linguiformis zones are often laminated and framboidal, indicating that anoxic

conditions were developed. Allochthonous fauna is contained within the common, thick sediment-gravity flows sourced from the nearby, better-oxygenated shelf.

Interestingly, the deep-water sections of the Woodruff Basin record marginally better oxygenation conditions than the deepest section of the Pilot Basin (Coyote Knolls). Thus dysoxic conditions, with weakly bioturbated strata, are recorded in the Late *rhenana* and *linguiformis* zones at the deep-water Warm Springs section (Figs. 15 and 16). The most intensely anoxic conditions in the basinal sections are recorded from the Early *rhenana* and latest Frasnian strata. If the Warm Springs section is the deepest record, it is possible that the floor of the Woodruff Basin was, for much of the F-F interval, around the lower limit of a mid-water oxygen minimum zone (Fig. 15). Intensification and expansion of this zone around the F-F boundary may be responsible for the basin-wide spread of anoxia at this time. Support for this oxygenation history comes from the even deeper water record of the Shoshone Mountains of northern Nevada. Here, the Slaven Chert records the quiet accumulation of biogenic silica in a “relatively distal or isolated location” (Boundy-Sanders et al., 1999). A Late *rhenana* Zone section of the Chert consists of abundant siliceous sponge spicules that indicate ample seafloor oxygen levels at this time (Boundy-Saunders et al., 1999). This is in marked contrast with the intensely oxygen-restricted deposition of contemporaneous slope sections studied here.

5.2. Comparison with inorganic geochemical data

The oxygenation history for the Pilot and Woodruff basins contrasts with that suggested by Bratton et al. (1999). They investigated the Whiterock Canyon and Coyote Knolls sections and estimated palaeo-oxygen levels on the basis of trace metal concentrations, principally vanadium. Based on a decrease in V concentration from 2663 ppm to just 284 ppm at Whiterock Canyon, Bratton et al. (1999, p. 282) suggested that within the *linguiformis* Zone “there is a dramatic shift to fully oxic Zone 1 conditions” around 40 cm below the F-F boundary. However, the rocks at Whiterock Canyon are intensely and deeply weathered, and it is likely that this has affected the trace metal content. Such weathering has no effect neither on the pyrite framboid distribution, nor the sediment fabric, which remains finely laminated throughout. The inferred palaeo-oxygenation history of Bratton et al. (1999) is not supported by the lithological and pyrite framboid data in this study, which indicates that anoxic conditions prevailed up to the F-F boundary in the Woodruff Basin.

Similarly, the oxygenation history inferred by Bratton et al. (1999) for the Pilot Basin (Coyote Knolls) contradicts that suggested by data in this study. On the basis of V concentrations, Bratton et al. (1999) suggested that the main anoxic pulse in the Pilot Basin ended 6 m below the F-F boundary, during the *linguiformis* Zone, and that conditions were fully oxygenated at the boundary. The presence of tiny framboids and fine lamination, and the absence of fossils in the boundary beds are contrary to this interpretation, and indicate that anoxia persisted up to the F-F boundary. Bratton et al. (1999) have a low sampling density in the *linguiformis* Zone, and it may be possible that their “oxic” samples were taken from the turbidite beds, and do not reflect conditions at the depositional site itself.

The clearest record of depositional conditions comes from those sections where high sedimentation rates and turbidite deposition have not hindered the assessment of background oxygen levels. In summary, conditions were oxygen restricted during much of the

Early *rhenana* to *triangularis* zones in both the Woodruff and Pilot basins (Fig. 16). Anoxia appears to have been most intense around the Early–Late *rhenana* Zone boundary, and again in the latest *linguiformis* zone, when euxinic conditions developed. These euxinic pulses are age-equivalent with the Kellwasser anoxic horizons in Europe and may be considered the Great Basin manifestation of these phenomena.

5.3. Oxygenation history on the shelf

No sections recording deposition in a shelf environment have been studied here and inferences can only be made on the basis of the allochthonous clasts sourced from this setting. The presence of a varied benthic shelf fauna entrained within sediment-gravity flows in the Devils Gate and Coyote Knolls sections suggests that, in general, the source area supplying carbonate clasts to the Pilot Basin was well-oxygenated. However, turbidites are not present in the critical, topmost *linguiformis* Zone interval at Devils Gate, and those from this interval at Coyote Knolls are not fossiliferous. This tentative evidence for shelfal anoxia provides a kill mechanism for the 75% extinction recorded amongst ostracod species from the Devils Gate sediment-gravity flows (Casier and Lethiers, 1998). Further indirect evidence for shallow-water anoxia near the F-F boundary is provided by the basal Famennian flat-pebble conglomerates in the Tempiute Mountain section, which are thought to have formed in response to the suppression of bioturbation by anoxia. The resultant thin-bedded carbonates have been eroded by storms to source the distinctive and unusual “flat pebbles” seen in the allodapic carbonates (see Wignall and Twitchett, 1999).

5.4. Event stratigraphy and sea-level change

Sandberg et al. (1997) identified a 20-event stratigraphy in the Middle and Late Devonian of Nevada and Utah. Of these, events 8 (major eustatic rise during the Early *rhenana* Zone), 9 (rapid eustatic rise and fall during the *linguiformis* Zone), and 10 (mass extinction at the F-F boundary) fall within the time frame of this study. Within the Early *rhenana* Zone in the Pilot Basin (Coyote Knolls), the carbonate platform is drowned and the Guilmette Formation is replaced by the Pilot Shale, evidence of a major deepening. This corresponds to a major eustatic rise, Event 8 of Sandberg et al. (1997), but could equally be the result of regional tectonic subsidence at this locality. The Devils Gate, Northern Antelope Range (Sandberg et al., 2003), and Tempiute Mountain (Morrow and Sandberg, 2003) sections also record evidence of deepening during the Early *rhenana* Zone, which gives evidence of the *semichatovae* transgression throughout the region.

Based on this study, there is little lithological evidence for Event 9 of Sandberg et al. (1997) because the lithology and facies around this level change little, or this crucial interval is not preserved. The sea-level curve of Sandberg et al. (2002) shows a sea-level fall throughout the late part of the *linguiformis* Zone. This is primarily based on the increased abundance of the normally shallow-water conodont genus *Icriodus*, from a minor component to as high as 30% of the total conodont fauna within previous deeper water settings (Sandberg et al., 1988).

Several sections record an increase in clastic content at or near to the F-F boundary (Fig. 17). At Coyote Knolls this is manifest as a change from calcisiltite to coarse siltstone. At Devils Gate, micrites and silty shales grade into siltstones in the boundary bed, but the lithology abruptly returns to carbonates for the remainder of the Early *triangularis* Zone. The Whiterock Canyon section records an influx of silt in the uppermost Frasnian and basal Famennian (Fig. 17). At Tempiute Mountain there is a marked change in lithology as micritic background sedimentation is replaced by thick, sandstone turbidites at the F-F boundary. These lithological changes are not seen everywhere, for example the clastic content in the Northern Antelope Range declines in the same interval (Fig. 17), but they have been used as evidence for a major sea-level fall beginning in the later part of the *linguiformis* Zone (Sandberg et al., 2002; Morrow and Sandberg, 2003). In this case, the intensification and peak of anoxia at the F-F boundary in the Great Basin would occur during a major regressive interval; this is an unusual occurrence because other major anoxic events of the geological record occur during transgression or highstand (e.g. Hallam and Wignall, 1997, 1999). However, the increased clastic content might not be related to sea-level changes at all, but could arise from a reduction in carbonate productivity on the shelf during the mass extinction or a climate change to increased humidity and the development of a mixed clastic-carbonate depositional system. We would argue that the evidence for a major regression at the end of the *linguiformis* Zone is not compelling.

Event 10 of Sandberg et al. (1997), the F-F mass extinction, is difficult to recognise in many of the studied sections (although the allochthonous fossils, such as corals (e.g. Sandberg et al., 1988), ostracods (e.g. Casier and Lethiers, 1998), and conodont faunas (e.g. Sandberg et al., 1988) clearly record major extinction steps at Devils Gate). The most notable crisis in the basinal sections is the temporary loss of radiolaria in the F-F boundary interval.

6. Anoxia as an extinction mechanism

Anoxia has long been regarded as one of the most likely kill mechanisms of the F-F mass extinction (e.g. House, 1985; Casier, 1987; Sandberg et al., 1988; Walliser et al., 1989; Goodfellow et al., 1989; Buggisch, 1991; Becker, 1993; Joachimski and Buggisch, 1993; Joachimski et al., 2001; Bond et al., 2004). Implicit in the anoxia kill hypothesis is the need for globally synchronous anoxia. The lack of a demonstrable synchronicity has been one of the key arguments against the mechanism (Becker et al., 1991; McGhee, 1996; Copper, 1998; Bratton et al., 1999; House, 2002). The principal support for the detractors has come from the Nevada and Utah sections where, as noted above, improved oxygenation has been reported from the F-F boundary (Bratton et al., 1999). However, our evidence suggests that anoxia prevailed and often intensified leading up to the F-F boundary in the Great Basin. The Upper Kellwasser anoxic event is thus seen to be present in the western United States, considerably strengthening the likelihood that it was the cause of the F-F mass extinction. However, the same cannot be said of the Lower Kellwasser event. Based on lithology and frambooid analyses, the Lower Kellwasser Horizon in Germany is within the early part of the Late *rhenana* Zone, whereas at Kowala Quarry in Poland, this anoxic event occurs much later, near the top of the Late *rhenana* Zone (Bond et al., 2004). Feist and Schindler

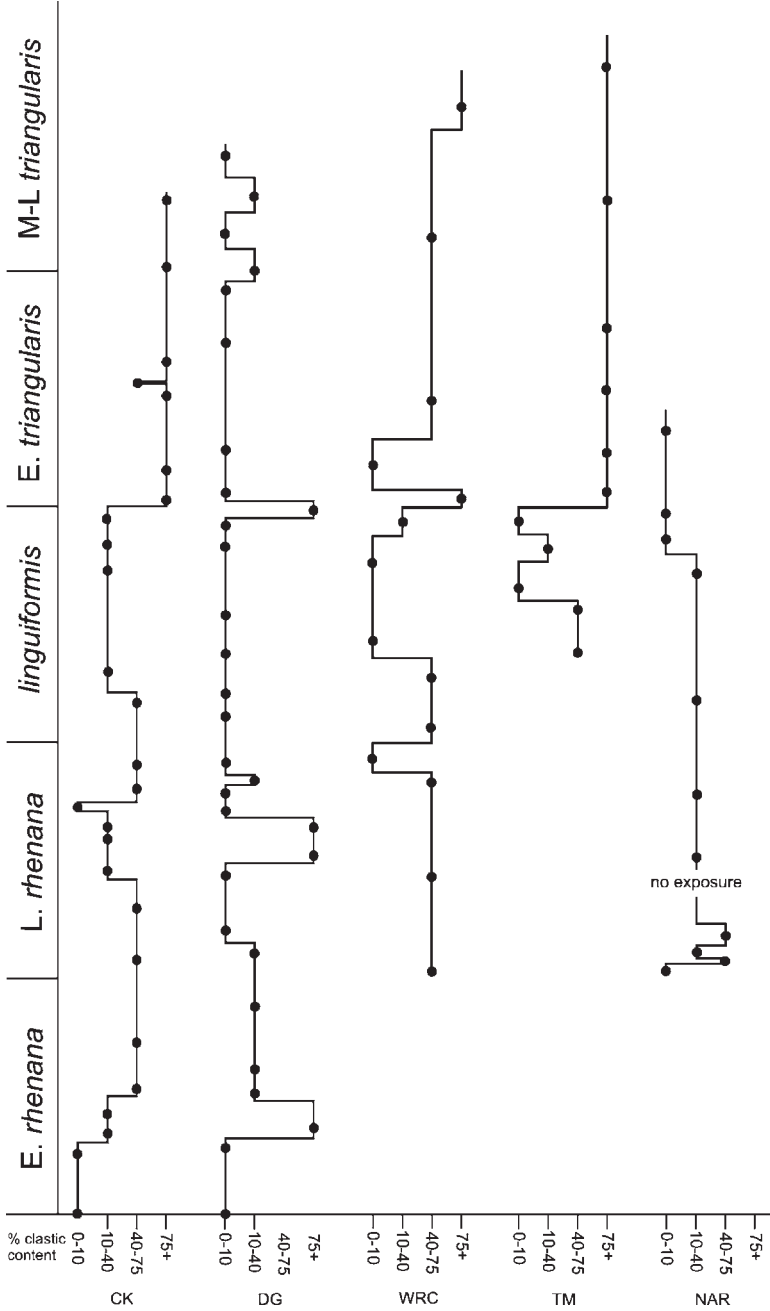


Figure 17. Summary of changes in clastic content in the F-F boundary sections of this study. These values are based on petrographic analyses. Data points are represented by nodes.

(1994) have previously noted a non-synchronicity between French and German developments of Lower Kellwasser “dark facies” based on lithology, as have Crick et al. (2002), based on magnetic susceptibility correlation data. Similarly, in the Great Basin, there is no clear, basin-wide increase in anoxic intensity at any level in the Late *rhenana* Zone and several deep-water sections seem rather well oxygenated at this time. Synchronicity is therefore the key difference between these two anoxic events – and an explanation as to why only the anoxic event during the latest *linguiformis* Zone saw catastrophic faunal losses, because at this time the extent of anoxia was at its peak extent both vertically and laterally within the water column.

Acknowledgements

We thank Jared Morrow for his invaluable field guidance and discussions during this project. He is also thanked, together with Michael Joachimski for their comments on an earlier version of the manuscript. Bond’s research was funded by a PhD studentship from the Natural Environment Research Council.

References

- Becker, R.T., 1993. Stratigraphische Gliederung und Ammonoiten-Faunen im Nehdenium (Oberdevon II) von Europa und Nord-Afrika. *Cour. Forsch.-Inst. Sencken.* 155, 1–405.
- Becker, R.T., House, M.R., Kirchgasser, W.T., Playford, P.E., 1991. Sedimentary and faunal changes across the Frasnian/Famennian boundary in the Canning Basin of Western Australia. *Hist. Biol.* 5, 183–196.
- Bond, D., Wignall, P.B., Racki, G., 2004. Extent and duration of marine anoxia during the Frasnian-Famennian (Late Devonian) mass extinction in Poland, Germany, Austria and France. *Geol. Mag.* 141, 1–29.
- Boundy-Sanders, S.Q., Sandberg, C.A., Murchey, B.L., Harris, A.G., 1999. A late Frasnian (Late Devonian) radiolarian, sponge spicule, and conodont fauna from the Slaven Chert, northern Shoshone Range, Roberts Mountains Allochthon, Nevada. *Micropaleontology* 45, 62–68.
- Bratton, J.F., Berry, W.B.N., Morrow, J.R., 1999. Anoxia pre-dates Frasnian-Famennian boundary mass extinction horizon in the Great Basin, USA. *Palaeogeogr. Palaeoclimatol. Palaeoecol.* 154, 275–292.
- Buggisch, W., 1972. Zur Geologie und Geochemie der Kellwasserkalke und ihrer begleitenden Sedimente (Unteres Oberdevon). *Geology and geochemistry of the lowermost Devonian Kellwasser Limestone and its associated sediments.* *Abhand. Hess. Landesamtes Bodenforsch.* 62, 1–67.
- Buggisch, W., 1991. The global Frasnian-Famennian ‘Kellwasser Event’. *Geol. Rund.* 80, 49–72.
- Canfield, D.E., Thamdrup, B., 1994. The production of ³⁴S-depleted sulphide during bacterial disproportionation of elemental sulfur. *Science* 266, 1973–1975.
- Casier, J.-G., 1987. Etude biostratigraphique et paléocéologique des ostracodes du récif de marbre rouge du Hautmont à Vodelée (partie supérieure du Frasnien, Bassin de Dinant, Belgique). *Rev. Paléobiol.* 6, 193–204.
- Casier, J.-G., Lethiers, F., 1998. Les Ostracodes du Frasnien terminal (zone à *linguiformis* des Conodontes) de la coupe du col de Devils Gate (Nevada, USA). Latest Frasnian (*linguiformis* conodont zone) ostracods from the Devils Gate Pass section, Nevada, USA. *Bull. L’Inst. Royal Sci. Nat. Belg. Sci. Terre* 68, 77–95.
- Casier, J.-G., Lethiers, F., Claeys, P., 1996. Ostracod evidence for an abrupt mass extinction at the Frasnian/Famennian boundary (Devils Gate, Nevada, USA). *Compt. Rend. l’Acad. Sci., Ser. II. Sci. Terre Planet.* 322(5), 415–422.
- Copper, P., 1998. Evaluating the Frasnian-Famennian mass extinction: comparing brachiopod faunas. *Acta Palaeont. Polon.* 43, 137–154.

- Crick, R.E., Ellwood, B.B., Feist, R., El Hassani, A., Schindler, E., Dreesen, R., Over, D.J., Girard, C., 2002. Magnetostratigraphy susceptibility of the Frasnian/Famennian boundary. *Palaeogeogr. Palaeoclimatol. Palaeoecol.* 181(1–3), 67–90.
- Droser, M.L., Bottjer, D.J., 1986. A semiquantitative field classification of ichnofabric. *Journ. Sed. Pet.* 56, 558–559.
- Feist, R., Schindler, E., 1994. Trilobites during the Frasnian Kellwasser Crisis in European Late Devonian cephalopod limestones. *Cour. Forsch.-Inst. Sencken.* 169, 195–223.
- Follmi, K.B., Grimm, K.A., 1990. Doomed pioneers: Gravity flow deposition and bioturbation in marine oxygen-deficient environments. *Geology*, 18, 1969–1972.
- Goodfellow, W.D., Geldsetzer, H.H.J., McLaren, D.J., Orchard, M.J., Klapper, G., 1989. Geochemical and isotopic anomalies associated with the Frasnian-Famennian extinction. *Hist. Biol.* 2, 51–72.
- Hallam, A., 1980. Black shales. *J. Geol. Soc. London* 137, 123–124.
- Hallam, A., Wignall, P.B., 1997. Mass extinctions and their aftermath. Oxford University Press, Oxford.
- Hallam, A., Wignall, P.B., 1999. Mass extinctions and sea-level changes. *Earth-Sci. Rev.* 48, 217–250.
- Hose, R.K., Armstrong, A.K., Harris, A.G., Mamet, B.L., 1982. Devonian and Mississippian rocks of the northern Antelope Range, Eureka County, Nevada. *US Geol. Surv. Prof. Paper* 1182, 19p.
- House, M.R., 1985. Correlation of mid-Palaeozoic ammonoid evolutionary events with global sedimentary perturbations. *Nature* 313(5997), 17–22.
- House, M.R., 2002. Strength, timing, setting and cause of mid-Palaeozoic extinctions. *Palaeogeogr. Palaeoclimatol. Palaeoecol.* 181(1–3), 5–26.
- Joachimski, M.M., Buggisch, W., 1993. Anoxic events in the late Frasnian – causes of the Frasnian-Famennian faunal crisis? *Geology* 21, 675–678.
- Joachimski, M.M., Ostertag-Henning, C., Pancost, R.D., Strauss, H., Freeman, K.H., Littke, R., Damste, J.S.S., Racki, G., 2001. Water column anoxia, enhanced productivity and concomitant changes in $\delta^{13}\text{C}$ and $\delta^{34}\text{S}$ across the Frasnian-Famennian boundary (Kowala – Holy Cross Mountains/Poland). *Chem. Geol.* 175(1–2), 109–131.
- Joachimski, M.M., Pancost, R.D., Freeman, K.H., Ostertag-Henning, C., Buggisch, W., 2002. Carbon isotope geochemistry of the Frasnian-Famennian transition. *Palaeogeogr. Palaeoclimatol. Palaeoecol.* 181, 91–109.
- Johnson, J.G., Klapper, G., Elrick, M., 1996. Devonian transgressive-regressive cycles and biostratigraphy, Northern Antelope Range, Nevada: establishment of reference horizons for global cycles. *Palaios* 11, 3–14.
- Johnson, J.G., Klapper, G., Sandberg, C.A., 1985. Devonian eustatic fluctuations in Euramerica. *Geol. Soc. Am. Bull.* 96, 567–587.
- Johnson, J.G., Klapper, G., Trojan, W.R., 1980. Brachiopod and conodont successions in the Devonian of the northern Antelope Range, central Nevada. *Geol. Palaeont.* 14, 77–116.
- Lüning, S., Kolonic, S., Loydell, D., Craig, J., 2003. Reconstruction of the original organic richness in weathered Silurian shale outcrops (Murzuq and Kufra basins, southern Libya). *Geoarabia* 8, 299–308.
- McGhee, G.R., 1996. *The Late Devonian Mass Extinction*. Columbia University Press, New York.
- Morrow, J.R., 1997. Shelf-to-basin event stratigraphy, conodont paleoecology, and geologic history across the Frasnian-Famennian (F-F mid-Late Devonian) boundary mass extinction, central Great Basin, western U.S. Boulder, Colorado. University of Colorado, Ph.D. dissertation, 355pp.
- Morrow, J.R., 2000. Shelf-to-basin lithofacies and conodont paleoecology across Frasnian-Famennian (F-F, mid-Late Devonian) boundary, central Great Basin (Western U.S.A.). *Cour. Forsch.-Inst. Sencken.* 219, 1–57.
- Morrow, J.R., Sandberg, C.A., 2003. Late Devonian sequence and event stratigraphy across the Frasnian-Famennian (F-F) boundary, Utah and Nevada. In: Harries, P.J. (Ed.), *High-Resolution Approaches in Stratigraphic Paleontology*. Kluwer Dordrecht, pp. 351–419.
- Muramoto, J.A., Honjo, S., Fry, B., Hay, B.J., Howarth, R.W., Cisne, J.L., 1991. Sulfur, iron and organic carbon fluxes in the Black Sea: sulfur isotopic evidence for origin of sulfur fluxes. *Deep-Sea Res.* 38, S1151–S1187.
- Peterhaensel, A., Pratt, B.R., 2001. Nutrient-triggered bioerosion on a giant carbonate platform masking the post-extinction Famennian benthic community. *Geology* 29(12), 1079–1082.
- Racki, G., Racka, M., Matyja, H., Devleeschouwer, X., 2002. The Frasnian/Famennian boundary interval in the South Polish-Moravian shelf basins: integrated event-stratigraphical approach. *Palaeogeogr. Palaeoclimatol. Palaeoecol.* 181, 251–297.
- Raiswell, R., 1982. Pyrite texture, isotopic composition and the availability of iron. *Am. J. Sci.* 282, 1244–1263.
- Raiswell, R., Newton, R., Wignall, P.B., 2001. An indicator of water-column anoxia: resolution of biofacies variations in the Kimmeridge Clay (Upper Jurassic, UK). *J. Sed. Res.* 71, 286–294.

- Raup, D.M., Sepkoski, J.J., 1982. Mass extinction in the marine fossil record. *Science* 215, 1501–1503.
- Sandberg, C.A., Morrow, J.R., Poole, F.G., Ziegler, W., 2003. Middle Devonian to Early Carboniferous event stratigraphy of Devils Gate and Northern Antelope Range sections, Nevada, U.S.A. *Cour. Forsch.-Inst. Sencken.* 242, 187–207.
- Sandberg, C.A., Morrow, J.R., Warme, J.E., 1997. Late Devonian Alamo impact event, global Kellwasser events, and major eustatic events, eastern Great Basin, Nevada and Utah. *Brigham Young Univ. Geol. Stud.* 42, 129–160.
- Sandberg, C.A., Morrow, J.R., Ziegler, W., 2002. Late Devonian sea-level changes, catastrophic events, and mass extinctions. In: Koeberl, C., MacLeod, K.G., (Eds), *Catastrophic Events and Mass Extinctions: impacts and Beyond*. *Geol. Soc. Am. Spec. Pap.* 356, 473–487.
- Sandberg, C.A., Poole, F.G., 1977. Conodont biostratigraphy and depositional complexes of Upper Devonian cratonic-platform and continental-shelf rocks in the western United States. In: Murphy, M.A., Berry, W.B.N., Sandberg, C.A. (Eds.), *Devonian of North America*. *Camp. Mus. Contrib.* 4, 144–182.
- Sandberg, C.A., Poole, F.G., Johnson, J.G., 1989. Upper Devonian of Western United States. In: McMillan, N.J., Embry, A.F., Glass, D.J. (Eds), *Devonian of the World*. *Can. Soc. Petrol. Geol. Memoir* 14(III), 183–220.
- Sandberg, C.A., Ziegler, W., Dreesen, R., Butler, J.L., 1988. Part 3: Late Frasnian mass extinction: conodont event stratigraphy, global changes, and possible causes. *Cour. Forsch.-Inst. Sencken.* 102, 263–307.
- Savrdá, C.E., Bottjer, D.J., 1986. Trace-fossil model for reconstruction of paleo-oxygenation in bottom waters. *Geology* 14(1), 3–6.
- Schindler, E., 1990. Die Kellwasser-Krise (hohe Frasn-Stufe, Ober Devon). *Gottinger Arbeiten zur Geol. Paläont.* 46, 1–115.
- Scotese, C.R., McKerrow, W.S., 1990. Revised world maps and introduction. *Mem. Geol. Soc. Lond.* 12, 1–21.
- Sepkoski, J.J., 1996. Patterns of Phanerozoic extinction: a perspective from global data bases. In: Walliser, O.H. (Ed.), *Global Events and Event Stratigraphy*, Springer-Verlag, Berlin, pp. 35–52.
- Walliser, O.H., 1996. Global events in the Devonian and Carboniferous. In: Walliser, O.H. (Ed.), *Global Events and Event Stratigraphy*. Springer-Verlag, Berlin, pp. 225–250.
- Walliser, O.H., Groos-Uffenorde, H., Schindler, E., Ziegler, W., 1989. On the Upper Kellwasser Horizon (boundary Frasnian/Famennian). *Cour. Forsch.-Inst. Sencken.* 110, 247–255.
- Wendt, J., Belka, Z., 1991. Age and depositional environment of Upper Devonian (early Frasnian to early Famennian) black shales and limestones (Kellwasser Facies) in the eastern Anti-Atlas, Morocco. *Facies* 25, 51–90.
- Wignall, P.B., Myers, K.J., 1988. Interpreting benthic oxygen levels in mudrocks – a new approach. *Geology* 16, 452–455.
- Wignall, P.B., Newton, R.J., 1998. Pyrite framboid diameter as a measure of oxygen deficiency in ancient mudrocks. *Am. J. Sci.* 298, 537–552.
- Wignall, P.B., Twitchett, R.J., 1999. Unusual intraclastic limestones in Lower Triassic carbonates and their bearing on the aftermath of the end-Permian mass extinction. *Sedimentology* 46(2), 303–316.
- Wilkin, R.T., Barnes, H.L., 1996. Pyrite formation by reactions of iron monosulfides with dissolved inorganic and organic sulfur species. *Geochim. Cosmo. Acta* 60, 4167–4179.
- Wilkin, R.T., Barnes, H.L., 1997. Formation processes of framboidal pyrite. *Geochim. Cosmo. Acta* 61, 323–339.
- Wilkin, R.T., Barnes, H.L., Brantley, S.L., 1996. The size distribution of framboidal pyrite in modern sediments: an indicator of redox conditions. *Geochim. Cosmo. Acta* 60, 3897–3912.
- Yudina, A.B., Racki, G., Savage, N.S., Racka, M., Malkowski, K., 2002. The Frasnian-Famennian events in a deep-shelf succession, Subpolar Urals: biotic, depositional and geochemical records. *Acta Palaeont. Polon.* 47, 355–372.

Appendix A Locality details

Coyote Knolls (39.47° N, 113.62° W)

This section is exposed in and above a T-shaped gully in Tule Valley, Millard County, western Utah (Fig. 5). This remote section can be accessed via a dirt track, 14.3 km north of the Cowboy Pass, which is a gravel road 50 km to the north of US Highway 50. The gully section lies at the bottom of a well-bleached scree slope, 5.5 km due west from Coyote Knolls (for more details see Sandberg et al., 1997). The gully exposes an almost unbroken F-F sequence of over 70 m thickness, dipping westwards, with the F-F boundary in the western wall of the gully. In total, our study records 43 beds.

Devils Gate (39.57° N, 116.07° W)

The base of the section is reached following Highway 50 for 13 km west from the town of Eureka. Shortly before the road passes through “Devils Gate”, a track (the old highway) branches off on the north side. After following this track for 300 m, the section begins in the hillside immediately to the north (for more details see Sandberg et al., 1997). The bed numbers of Sandberg et al. (1988) are painted on several of the beds, but are not followed here. In total, our study comprises 42 beds.

Northern Antelope Range (NAR-A = 39.24° N, 116.24° W)

This location is a composite of two separate sections, NAR-A and -B. NAR-B, a steep slope section, is stratigraphically lower and is the easiest section to access. It can be reached following the main dirt road on the eastern side of the Antelope Valley, which runs several miles south of US Highway 50. Shortly before a cattle grid and fence meet the road, a rough track leads off to the southeast, into the range. After approximately 2 km this track ends, and the NAR-B section is exposed in a cliff and hillside. NAR-A is exposed in a cliff section some 1000 m to the north. In total the two sections expose a F-F boundary sequence almost 70 m thick, comprising 26 beds. A map of the locality is also given in Morrow (1997).

Tempiute Mountain (37.62° N, 115.64° W)

The section can be accessed by exiting Highway 375 on a dirt road 4.8 km northwest of Coyote Summit, to the east of the town of Rachel. Driving north, after 2.2 km, take the left fork, and continue northwest for 2.2 km to a gate in the canyon between Tempiute Mountain and Chocolate Drop. After parking by this gate, the section can be reached by walking up the canyon and joining an old mine footpath which runs to the southwest. Skirting round the summit, the section lies on the western side of the mountain at an elevation of approximately 7800 ft. In total, our study includes 15 beds. A map of the locality is also given in Morrow (1997).

Whiterock Canyon (37.62° N, 115.64° W)

This section is accessed by exiting Highway 50 southwards on the Antelope Valley road, 32 km west of Eureka. This road runs along the valley floor towards Segura Ranch. After 36 km, shortly before the ranch, take Forest Road 025 westwards into the Monitor Range. After a further 7 km, a track leads off the Forest Road southwards into Copenhagen Canyon. After 5 km take a fork westwards, past Rabbit Hill to the north, and into Whiterock Canyon, towards Horse Heaven Mountain. Following this track to the end, the section can be reached by walking a further kilometre west. The section, which comprises 13 beds, lies in trenches dug into a scree slope on the north side of the canyon. A map of the locality is also given in Morrow (1997).

Warm Springs (38.18° N, 116.39° W)

The section is reached by following Highway 6 for 4.1 km south from the T-junction by the abandoned Warm Springs station. Parking by the highway, behind a knob of volcanic rocks, walk 500 m to the north along a track into a small, narrow canyon. The studied section, which comprises eight beds, is exposed in the western wall of the canyon. The bed numbers of Sandberg et al. (1997) are painted on several of the beds, but are not followed here.

Appendix B

Pyrite framboid data (N = number in sample, SD = standard deviation, FD = framboid diameter (μm)).

Zone	Bed	N	Mean	SD	Max. FD	Min. FD
Coyote Knolls						
Early <i>rhenana</i>	9	110	4.3	1.4	9.5	1.5
Late <i>rhenana</i>	13	7	5.6	2.7	11.0	3.5
	17	104	5.4	2.6	15.5	2.5
	18	6	4.8	1.7	8.0	3.5
	19	95	5.3	2.0	12.0	2.5
	22	103	4.8	1.6	10.0	1.5
<i>linguiformis</i>	27	88	5.0	2.0	11.5	2.0
	29	106	3.7	1.3	7.0	1.5
	30	99	4.3	2.0	12.5	1.5
	31	67	4.5	1.8	12.5	2.0
	33	85	4.5	2.2	14.0	2.0
Early <i>triangularis</i>	35	64	6.6	3.9	22.0	2.5
	39	65	6.1	2.9	23.0	2.5
Devils Gate						
Early <i>rhenana</i>	2	17	6.0	2.1	10.0	3.0
	4	90	5.6	2.0	13.0	2.5
	5 (top)	77	5.3	2.0	11.0	2.0
	6 (top)	24	5.6	1.9	9.0	3.0
Late <i>rhenana</i>	7 (mid)	103	3.8	1.2	7.5	1.0
	11	69	5.4	2.0	16.0	3.0
	12	12	5.0	1.8	8.0	2.5
	15	13	4.2	1.1	7.0	3.0
<i>linguiformis</i>	26	95	5.1	1.4	9.5	2.5
	28 (top)	28	4.9	1.9	10.0	2.5
	29 (mid)	114	4.4	1.7	12.5	2.0
Early <i>triangularis</i>	30 (top)	47	4.0	1.0	7.0	2.5
	31	47	3.7	1.2	7.0	1.0
	34	40	4.5	2.1	12.0	2.0
Late <i>triangularis</i>	38	17	5.4	1.6	8.0	3.0
Tempiute Mountain						
<i>linguiformis</i>	5	4	3.5	0.4	4.0	3.0
	6	3	4.0	1.0	5.0	3.0
	7	8	5.1	1.7	8.5	3.5
Early <i>triangularis</i>	9	2	10.3	3.9	13.0	7.5
Late <i>triangularis</i> – <i>crepida</i>	14	57	6.8	1.9	12.5	4.0

Appendix B (*Continued*)

Zone	Bed	<i>N</i>	Mean	SD	Max. FD	Min. FD
Whiterock Canyon						
Late rhenana	1 (top)	81	5.3	2.2	14	2.5
	2 (mid)	80	4.9	1.9	11	1.5
	3 (mid)	95	4.5	2.1	17	2
linguiformis	4 (top)	98	4.2	1.6	9.5	2
	5 (mid)	74	6.2	2.3	12.5	2.5
	5 (top)	87	6.1	4.3	40	2
	6 (top)	100	5.5	2.0	14	2
Early–Mid triangularis	7	85	6.8	2.9	16	3
	8 (mid)	40	6.2	2.1	14.5	3.5
	9	52	4.9	1.6	8.5	2.5
Mid–Late triangularis	10 (top)	106	4.8	1.7	11	2
Warm Springs						
Early rhenana	3	4	6.4	1.4	7.5	4.5
Late rhenana– linguiformis	5	17	5.9	1.3	8.5	3.5
	6	10	5.7	1.2	7.5	4.5
F-F boundary	7	118	4.6	1.6	10.0	2.0